Copy
RM E56D16

5

Copy 2

RESEARCH MEMORANDUM

PERFORMANCE OF A SHORT TURBOJET COMBUSTOR WITH HYDROGEN FUEL IN A QUARTER-ANNULUS DUCT AND COMPARISON WITH PERFORMANCE IN A FULL-SCALE ENGINE

By Robert Friedman, Carl T. Norgren, and Robert E. Jones

Lewis Flight Propulsion Laboratory
Cleveland, Ohio

NATIONAL ADVISORY COMMITTEE
FOR AERONAUTICS
WASHINGTON
July 2, 1956

NATIONAL ADVISORY COMMITTEE FOR AERONAUTICS

RESEARCH MEMORANDUM

PERFORMANCE OF A SHORT TURBOJET COMBUSTOR WITH HYDROGEN FUEL IN A QUARTER-ANNULUS DUCT AND COMPARISON WITH PERFORMANCE IN A FULL-SCALE ENGINE

By Robert Friedman, Carl T. Norgren, and Robert E. Jones

SUMMARY

A number of short turbojet combustor configurations for hydrogen fuel were designed and their performance investigated in a quarter-annulus duct. The best combustor liner consisted of an annular primary zone and a secondary zone composed of T-shaped channels sloping from the primary zone to the combustor wall. The fuel manifold consisted of two concentric spray bars within a V-gutter flameholder with separate fuel connections to either spray bar for control of the initial fuel distribution. The distance from the fuel injectors to the instrumentation plane was 19.4 inches.

The quarter-annulus combustor operated at combustion efficiencies of 84 percent or greater at combustor-inlet total pressures as low as 5.7 inches of mercury absolute. Combustor reference velocity had little effect on combustion efficiency even at velocities as high as 270 feet per second. At a reference velocity of 80 feet per second, combustor total-pressure loss ranged from 3.0 percent of combustor-inlet total pressure at isothermal conditions to 4.7 percent at a combustor total-temperature ratio of 3.6.

The quarter-annulus combustor for hydrogen fuel was also scaled to fit a production-type, full-scale engine. This combustor was about two-thirds the length of the standard combustor for this engine. Combustion efficiency and total-pressure loss of the full-annulus combustor were approximately the same as those determined in the quarter-annulus duct. Desirable outlet-temperature profiles were obtained by controlling the fuel distribution to separate manifolds of a dual fuel manifold.

INTRODUCTION

Hydrogen fuel offers advantages for the airplane in that (1) the high heat release per pound of this fuel can greatly increase the operational

range of jet-powered aircraft (refs. 1 and 2), and (2) at the high stagnation temperatures associated with high flight speeds, the high heat capacity of this fuel furnishes a large heat sink for cooling portions of the engines and airframe, especially when the fuel is carried as a liquid (ref. 3). To obtain the gains in flight range that are possible with hydrogen, it is necessary to fly at higher altitudes than with conventional fuels (ref. 4). High-altitude flight requires a light-weight, high-thrust powerplant with a combustor capable of operating at low pressures. Fortunately, the high flame speed and wide inflammability limits of hydrogen permit efficient burning at very low pressures (refs. 3 and 5). These favorable combustion characteristics of hydrogen may also allow a decrease in burner length and consequently a decrease in engine weight.

Improvements in combustor performance through the use of hydrogen have already been demonstrated in current production-type combustors (refs. 6 and 7). The fullest advantages, however, would be realized in combustors designed specifically for hydrogen. The requirements for such combustors and a proposed design of an engine for hydrogen fuel were presented in a recent NACA conference (ref. 4). The proposed combustor is shorter than standard combustors and uses a simple low-pressure-drop liner, since a greater tolerance in the means of introduction of fuel and air is possible than with hydrocarbon fuel combustors.

The objective of the research program described herein was to demonstrate some design principles for a short-length, hydrogen-burning combustor. Subsequent evaluation in a full-scale, production-type engine was conducted at the NACA Lewis laboratory. Although a satisfactory design was found in the limited time available for the investigation, this configuration does not necessarily represent the best design that can be reached through more exhaustive tests of individual components of the combustor. The hydrogen-burning combustor was approximately two-thirds the length of the combustor currently used in the full-scale engine. The combustor walls were constructed of sloping, channel-shaped pieces to permit adequate mixing of primary combustion products and secondary air in a short length without undue total-pressure loss (ref. 8). In addition, the use of channels promises to be one of the more effective methods of increasing combustor life at supersonic flight conditions. Various fuel-injector designs were investigated, all of which consisted of simple, concentric spray bars.

A one-quarter sector of the annular combustor was operated at both low pressures and pressures above atmospheric. Combustion efficiency and total-pressure drop were determined over a range of velocities, with particular emphasis on conditions at low total pressures. Provisions were made to vary the outlet-total-temperature profile, and examples showing the control of the profile are described in this report. A comparison of the performance of the quarter-annulus model with that of the full-scale hydrogen-fuel combustor is also shown.

[redacted]

APPARATUS

Combustor Installation

A schematic diagram of the combustor installation is shown in figure 1. Air of the desired quantity and pressure was drawn from the laboratory air-supply system, metered with a sharp-edged orifice, passed through the combustor, and exhausted into the altitude exhaust sytem. A direct-fired preheater in the inlet plenum chamber was used to increase the combustor-inlet temperature for a few of the test runs.

Fuel-System Installation

A schematic diagram of the hydrogen-fuel system is shown in figure 2. The fuel was commercial hydrogen with a purity of about 98 percent. It was supplied in compressed-gas trailers consisting of banks of 22 to 37 gas cylinders loaded to a pressure of 2400 pounds per square inch. Each cylinder held about 1200 cubic feet, or 6.8 pounds, of hydrogen (at standard conditions). One or more cylinders were connected by manifolds as necessary. The desired quantity of fuel was taken from the cylinders, reduced to a working pressure of 50 to 150 pounds per square inch gage, metered with a sharp-edged orifice, and then injected into the combustor through a single- or dual-entry fuel manifold.

Safety precautions included use of an over-pressure relief valve set at 200 pounds per square inch, room and roof vents, and isolation of the operators' control room from all components of the fuel system.

Combustor

The combustor consisted of a one-quarter sector of an annular combustor designed to fit into a housing with an outside diameter of 25.5 inches and an inside diameter of 10.8 inches. The distance from the fuel injector to the exhaust instrumentation plane was approximately 19.4 inches, 25 percent shorter than previous experimental combustors that fit the same housing (ref. 8). The maximum combustor cross-sectional area of the quarter sector was 105 square inches (420 sq in. for the complete combustor).

A three-quarter-cutaway view of the final combustor model is shown in figure 3, and a longitudinal cross-sectional view in figure 4. Except for a minor modification in the secondary zone, all the configurations used the same combustor liner. The combustor consisted of an annular primary zone with a row of 5/8-inch-diameter holes in the inner wall only, a secondary zone composed of sloping channel-shaped pieces, and a heat shield located near the turbine-inlet section. These channels were each connected by perpendicular struts to metal liners that were bolted to the

inner and outer walls of the combustor. For ease of assembly and alinement this arrangement was preferred over the individually placed channels of reference 8.

The fuel manifolds shown in figures 3 and 4 are described in the discussion of combustor configurations. Ignition was provided by a conventional jet-engine spark plug with an extended shroud and electrode, mounted near the junction of the secondary channels and the primary annulus.

Instrumentation

The instrumentation stations are shown in figure 1. Combustor-inlet total temperature and total pressure were measured at station 1 with four bare-wire, chromel-alumel thermocouples and four total-pressure tubes, respectively. Combustor-outlet temperatures and pressures were measured at station 2 with a combined total-pressure and platinum-13-percent-rhodium - platinum thermocouple probe in a polar-coordinate traversing mechanism. A detailed description of this surveying method is given in reference 9. A two-pen X-Y recording potentiometer connected to the survey system continuously recorded outlet temperatures and total-pressure differential across the combustor. Static-pressure taps were also located at stations 1 and 2.

Combustor Configurations

A total of over 25 combustor configurations were investigated. Cross-sectional views of the primary or secondary zones of the eight most promising models are shown in figures 5(a) to (h). These eight models all had the channeled-wall liner shown in figures 3 and 4. The fuel manifolds for these configurations consisted of single or double concentric spray bars, perforated with 1/16- or 5/64-inch holes drilled as shown in figures 5(a) to (h). The small holes provided a moderate pressure drop and a uniform gas flow from all the orifices. At the same time, the injection pressure drop was low enough to allow the fuel jets to break up and mix with air before they penetrated an appreciable distance.

Model 1 (fig. 5(a)) was the simplest fuel-manifold configuration investigated. It consisted of a single fuel manifold concentric to the annular primary-zone walls, placed within a 90-degree V-gutter flameholder. The V-gutter blocked approximately 70 percent of the primary-zone cross-sectional area and created an eddy region for fuel-air mixing at the fuel injector. In model 2 (fig. 5(b)) two fuel-manifold and V-gutter combinations were used, instead of the single manifold of model 1.

In the succeeding configurations, the fuel manifolds were placed between two V-gutters with slightly different angular openings, displaced from one another longitudinally leaving narrow slots (usually 1/8 in.) between the two V-gutters from which the fuel flow emerged. More fuel orifices were drilled to increase the over-all orifice area and reduce the average fuel velocity out of the manifold. Model 3 (fig. 5(c)) had a single fuel manifold within the two V-gutters and metal strips normal to the air flow welded to the upstream V-gutter to create additional turbulence at the fuel injector. Model 4 (fig. 5(d)) lacked these blocking strips but had two fuel manifolds within the V-gutters. The manifolds were flattened tubes tacked together along the flattened sides. Thus, the single manifold of model 3 could be replaced by the two manifolds. With separate fuel entries to the two manifolds and external valves (fig. 2), the distribution of fuel to the two manifolds could be controlled as desired.

Models 5 to 8 were all modifications retaining the dual-fuel-manifold and double-V-gutter configuration of model 4. In model 5 (fig. 5(e)), the blocking strips were reinstalled, and a fine screen was placed over the fuel orifices to break up the fuel jets and promote a more uniform flow of gas out of the slots between the trailing edges of the two V-gutters. Model 6 (fig. 5(f)) had the same blocking strips as model 5, but these were extended to the outer combustor wall by three radial tabs, leaving three radial air passages in the outer annulus instead of the annular opening of model 5. Model 7 (fig. 5(g)) had in addition two tabs extending to the inner combustor wall, staggered with respect to the existing tabs in the outer annulus. The radial primary-air passages of models 6 and 7 permitted more uniform radial outlet-temperature profiles than the annular air passages of models 3 and 5. Model 8 (fig. 5(h)) was identical to model 7, except that a portion of the openings between the channels along the inner radius of the combustor liner was blocked by a 1-inch metal strip as a further aid to mixing within the combustor.

PROCEDURE

Range of Conditions

Combustor performance was evaluated over a range of fuel-air ratios at the following conditions:

Inlet-air total pressure, in. Hg abs	Air-flow rate, lb/sec	Inlet-air total temperature, °F	Reference velocity,[a] ft/sec	Simulated altitude, ft
32.6	4.815	80	84.1	53,500
14.7	1.878	80	72.6	70,000
9.01	1.172	80	74.1	80,000
5.65	.754	80	75.1	90,000

[a]Based on combustor maximum cross-sectional area of 0.73 sq ft (1/4-annulus) and combustor-inlet total conditions.

Except for temperature, these conditions represent present-day engines operating with annular combustors at a sea-level-static compressor total-pressure ratio of 6.8 and a Mach number of 0.9. Combustor-inlet air was at room temperature because of the difficulty of operating the preheater under low-pressure conditions. Several of the configurations were operated only at the most severe inlet-air total pressure of 5.65 inches of mercury absolute. Combustor models 7 and 8 were also operated at the following additional conditions:

Inlet-air total pressure, in. Hg abs	Air-flow rate, lb/sec	Inlet-air total temperature, °F	Reference velocity, ft/sec
15.0	1.90	850	174
15.0	2.40	850	215
15.0	2.97	850	260
46.0	9.12	900	270
55.0	9.12	900	230

The first three conditions were chosen to determine the effect of higher velocities at a subatmospheric pressure, and the last two simulated operation at flight Mach numbers of approximately 3.0 at an 80,000-foot altitude. Under these conditions, it was possible to use the direct-fired preheater (fig. 1) to obtain higher inlet-air temperatures. To produce an inlet-air temperature of 900° F, the preheater reduced the oxygen content of the inlet air from 21 to 17 percent.

Calculations

Combustion efficiency was calculated as the percentage ratio of actual to theoretical increase in enthalpy from the combustor-inlet instrumentation plane to the combustor-outlet traversing probe (stations 1

to 2, fig. 1) by using the method of reference 6. Combustor-inlet enthalpies were determined from a chart similar to that presented in reference 6, based upon a constant fuel-inlet temperature of 70° F. A value of 51,571 Btu per pound was used for the lower heat of combustion of hydrogen.

The reference velocities were calculated from the total pressure and temperature at the combustor-inlet instrumentation plane and the maximum cross-sectional area of the combustor (0.73 sq ft).

4064

The combustor total-pressure drop was determined by a direct measurement of the difference between the total pressure at the combustor-inlet and -outlet instrumentation planes. At low total-pressure levels, a water U-tube manometer was used for measurements; at higher total-pressure levels, the pressure pickup of the combustor-outlet survey system was used to record the total-pressure loss directly on the combustor-outlet survey chart.

RESULTS AND DISCUSSION

A summary of the results of the performance of the short combustor with hydrogen fuel is given in table I.

Preliminary Designs

The eight combustor configurations presented in this report were the most promising models out of a total of 25 investigated and represent successive steps in the design of a satisfactory short combustor. The design was based upon use of the channeled-wall secondary zone. In this construction, air is admitted by means of long slots, which facilitate the mixing in a relatively short length of the hot combustion products with the cooler diluent air. In addition, the channeled design shows promise of providing a more durable liner construction that is reasonably free from warping when the combustor is operated at higher heat-release rates.

An early design in this program used a combustor liner composed solely of the secondary-zone channels. The fuel was injected by means of simple spray bars. Even with the highly reactive hydrogen, however, the combustor encountered flame-out at pressures below 9 inches of mercury absolute. A sheltered primary zone was added to the channeled liner to provide a low-velocity region around the fuel manifold. The most suitable primary liner consisted of a solid basket, enclosing 20 percent of the annular cross-sectional area and perforated with a row of holes in the inner wall only. This basic combustor liner design was retained throughout this investigation with only minor modifications, while research was conducted in an effort to improve the fuel manifold design.

In the eight combustor configurations presented in this report, the fuel manifold consisted of a combined fuel-spray bar and V-gutter flameholder. The V-gutters created eddy regions for flame stabilization; and, since the combustor volume allotted to the primary combustion zone was relatively small, the design of these flameholders was found to be of prime importance to combustor performance.

Selection of Best Configurations

Combustion efficiencies of the eight combustor models are compared in figure 6 at the severe operating conditions of an inlet-air total pressure of 5.7 inches of mercury absolute, an inlet-air total temperature of 80° F, a reference velocity of 80 feet per second, and a fuel-air ratio of 0.0066. Because model 3 was not operated at lower fuel-air ratios, the efficiency for this configuration is shown at a fuel-air ratio of 0.0085. For the first two configurations, efficiency was better for model 2, which had a greater radial spread of fuel at the fuel injector. All the succeeding configurations employed the same basic flameholder design, consisting of one V-gutter located inside another V-gutter. For these combustors, efficiency was better with the models that had the blocking strips and tabs on the upstream V-gutter (models 3, 5, 6, 7, and 8). These blocking tabs and strips created low-velocity recirculation zones in their wakes and provided flame seats for those parts of the fuel-air mixtures that flowed upstream into these wakes. Also, the additional turbulence created by the blocking pieces may have aided the fuel and air mixing in the primary zones and improved combustion efficiency.

The most uniform temperature profiles were obtained with those configurations that had a dual fuel manifold, possibly because the use of the dual manifold resulted in a more uniform flow of fuel from all the fuel orifices. This difference is quite evident in figure 7, where the radial outlet-temperature profile of a single-fuel-manifold combustor, model 3, is compared with those of the dual-fuel-manifold combustors (models 6, 7, and 8) operated with equal fuel flow to both manifolds. The abscissa in this figure represents the distance along a turbine rotor blade positioned at the combustor-outlet instrumentation plane from blade root (inner radius) to tip (outer radius). The temperature points are circumferential averages at five radial positions taken from the survey-probe records; the method is illustrated in reference 9. The over-all average combustor-outlet total temperatures for the four models illustrated were not the same, ranging from 1528° F for model 3 to 1226° F for model 6, but the general shape of the profiles is sufficient for comparison.

On the basis of these comparisons, the most satisfactory performance with respect to combustion efficiency and combustor-outlet radial temperature profile was obtained with models 7 and 8. Model 6, however, was

used as a basis for the design of a full-scale annular combustor investigated at the NACA Lewis laboratory, results of which are presented later in this report for comparisons with the performance of the quarter-annulus combustor. Models 7 and 8 were modifications investigated in the quarter-annulus installation after the full-scale combustor had been constructed and operated. Most of the performance results presented in this report are for model 7, because this combustor configuration was investigated more extensively than was model 8. Combustion efficiencies of model 7 were slightly higher than those of model 6, and in turn, efficiencies of model 8 were slightly higher than those of model 7 (table I).

Performance of Best Models

Combustion efficiency. - A plot of the combustion efficiency of models 7 and 8 as a function of fuel-air ratio is shown in figure 8 for an inlet-air total pressure of 5.7 inches of mercury absolute, a reference velocity of 80 feet per second, and an inlet-air total temperature of 80° F. Lines of constant total-temperature rise across the combustor are also shown in this figure, plotted as a function of combustion efficiency and fuel-air ratio. It is noted that the hydrogen fuel-air ratios shown in figure 8 are only about one-third of those required with conventional liquid hydrocarbon fuels for the same values of total-temperature rise.

With increasing fuel-air ratio, combustion efficiency decreased slightly, as shown in figure 8. A similar trend was also noted in a study where hydrogen fuel was tested in production-type combustors (ref. 6). The decrease in combustion efficiency was attributed to overenrichment of the primary zone, since the production-type combustors were designed for liquid hydrocarbon fuels and were provided with a large, shielded primary zone and allowed a very gradual air admission along the combustor length. The overenrichment was corrected to a certain extent in the experimental combustors for hydrogen fuel by a short primary zone and rapid introduction of secondary air beyond the primary zone.

With the dual-fuel-manifold configurations, models 4 to 8, it was possible to direct more fuel toward the outer or inner wall of the combustor as desired. This arrangement was intended for control of combustor-outlet temperature profiles, but assurance was necessary that these manipulations could be made without a great sacrifice in efficiency. Accordingly, the effect of fuel distribution on combustion efficiency of models 6 and 7 was determined. The results are shown in figure 9 at the same severe operating conditions used in the comparison of efficiency of the combustor configurations (fig. 6). The relative proportion of fuel to the inner and outer spray bars of the dual fuel manifolds, based upon valve settings, is the abscissa for this figure. Model 6 is included because this configuration was operated over a complete range of valve settings. Although a balanced distribution of fuel to both fuel manifolds

gives somewhat higher efficiencies, the attainment of a prescribed outlet-temperature profile is important enough to justify operation at other fuel distributions at a slight decrease in combustion efficiency.

Combustion efficiency of model 7 as a function of fuel-air ratio at several combustor-inlet pressures is shown in figure 10. For an inlet-air total pressure of 5.7 inches of mercury absolute, combustion efficiency was about 84 percent at fuel-air ratios of 0.0070 to 0.0090, increasing at lower fuel-air ratios to 92 percent at 0.0037. For a total pressure of 9.0 inches of mercury, efficiency increased from 90 percent at a fuel-air ratio of 0.0083 to 96 percent at 0.0040. At higher pressures, combustion efficiency ranged between 95 and 100 percent, as shown by the curve for a pressure of 30 inches of mercury.

The effect of combustor reference velocity on combustion efficiency at a constant fuel-air ratio and combustor-inlet temperature is shown in figure 11. Combustion efficiency at reference velocities from 75 to 155 feet per second is shown for model 7 at pressures of 5.7 and 9.0 inches of mercury absolute. Additional data are shown for model 8 at reference velocities of 230 to 270 feet per second and a pressure level of 47 to 55 inches of mercury (supersonic flight conditions). At all these conditions, combustion efficiency was virtually independent of reference velocity.

For a simulated flight altitude of 80,000 feet and an engine with a pressure ratio of 4.2, the combustor-inlet conditions of temperature, pressure, and velocity were related to a flight Mach number. The combustion efficiencies at these inlet conditions are plotted as a function of the calculated Mach number in figure 12. As Mach number increased at a given altitude, combustion efficiency approached a maximum, principally because of the increase in combustor-inlet pressure, although temperature and velocity also increased. The same trend is illustrated in figure 12 for an experimental channeled-wall combustor operated with liquid JP-type fuel (data from ref. 4, p. 45, based on ref. 8). The short combustor operated efficiently with hydrogen at lower Mach numbers, or more unfavorable inlet conditions.

The improvement in combustion efficiency with increase in combustor-inlet pressure for the experimental combustor is in accordance with the usual experience with turbojet combustors, but the performance with respect to velocity requires some explanation. For combustors where the oxidation of the fuel is assumed to be the controlling step in the overall combustion process, combustion efficiency has been correlated by the parameter pT/V (ref. 10), where p is combustor-inlet static pressure, T is combustor-inlet static temperature, and V is combustor reference velocity. Although the short hydrogen-fuel combustor was not operated over a complete range of all these conditions, nevertheless it is evident that the correlation does not apply with respect to velocity, since

efficiency did not decrease with increasing velocity (fig. 11). Hydrogen, which has a low activation energy and high flame speed, apparently has sufficient residence time to complete the oxidation and flame-propagation phases of the combustion process even in this short combustor at high velocities. It is more likely that the mixing of the fuel and air and the propagation of the flame through this mixture are the rate-controlling mechanisms in the combustor. Some evidence for this hypothesis is given by the increased efficiencies at low pressure with model 8 (fig. 8), where the change in the secondary-zone openings (fig. 5(h)) probably caused a redistribution of air to the primary zone with increased mixing in that zone. However, if the combustor length is further reduced, or if the flow velocity is further increased, a condition may eventually be reached where the fuel-air residence time in the combustor is so short that the chemical reaction may have insufficient time to go to completion, even with hydrogen fuel. At such a condition, an adverse effect on efficiency would be expected when velocity is increased. For the combustor described in this report, this point is apparently not reached for velocities as high as 270 feet per second.

Combustor-outlet total-temperature profiles. - An example of the radial-temperature-profile control possible through variation in the proportioning of fuel to the dual manifold is illustrated in figure 13, where combustor-outlet total-temperature profiles are shown for model 6 at an over-all average outlet total temperature of about 1100° F. As the fuel distribution was shifted from the outer to the inner manifold, the peak temperatures in the outlet profile shifted from the outer radius toward the inner radius. Thus, by appropriate control of the fuel flow to the manifold, a desired type of outlet-radial-temperature profile could be obtained. As shown in figure 9, these fuel-distribution manipulations have a slight effect on the combustion efficiency.

The same radial-temperature profile control was obtainable with the optimum configurations, models 7 and 8, although they were not operated over as complete a range of fuel-flow distributions as model 6. The radial temperature distribution shown in figure 14 is typical of those obtained for model 7. This profile is the result of a fuel distribution of about 80 percent to the outer manifold, and it shows a reasonable spread of 250° F at an average outlet total temperature of 1445° F.

Combustor total-pressure loss. - The channeled-wall design characteristically has a low total-pressure loss (ref. 8), but a slight increase in pressure loss had to be suffered in order to gain the benefits of the eddy-promoting blocking tabs in models 7 and 8. The total-pressure loss, in percent of combustor-inlet total pressure, is plotted for these models in figure 15 as a function of combustor total-temperature ratio. Data were taken at inlet-air total pressures from 5.7 to 30 inches of mercury absolute and a reference velocity of about 80 feet per second.

[redacted]

Because of the difficulty in making precise pressure-difference measurements at the low total-pressure levels, there is considerable scatter in the data. Pressure loss varied from approximately 3.0 percent at a total-temperature ratio of 1.0 (isothermal conditions) to 4.7 percent at a temperature ratio of 3.6. Agreement of the data points for model 8 and the faired curve is fortuitous.

Comparison with Full-Scale Combustor

Design of combustor. - Combustor model 6, and later models 7 and 8, were used as bases for the design of a full-scale annular combustor for hydrogen fuel. This combustor was fitted into a current, production-type engine in the 8000-pound-thrust class. Because of the convenience of using existing quarter-annulus ducting, the combustor was first investigated in the installation described in this report, even though the dimensions of the sector did not correspond to those required for the full-scale engine. It was thus necessary to scale the combustor to fit not only a larger annulus but also an annulus having a larger mean radius. The channeled-wall type of design, however, lent itself particularly well to this scaling. The shortened combustor was approximately two-thirds the length of the production-type combustor it replaced, but it had to occupy the standard combustor housing in the engine. Thus while the downstream end of the combustor fit against the turbine-nozzle diaphragm, there was an unoccupied gap between the upstream end of the combustor and the compressor outlet. Fuel-line and spark-plug entries were modified to accommodate the requirements of the shortened combustor liner.

Photographs of the full-scale combustor are shown in figure 16. The pictures were taken looking upstream from the turbine-nozzle diaphragm. The enlarged view, figure 16(a), shows the downstream V-gutter of the flameholder and the slot between the V-gutters from which the fuel emerges. The inner- and outer-radius channels, connecting struts, inner liner, and the downstream heat shield can also be seen.

Combustion efficiency. - Combustion efficiency of the quarter-annulus models agreed with those obtained in the full-scale engine within 5 percent at all conditions.

Combustor-outlet total-temperature profile. - Normally engine test installations carry temperature instrumentation only at the turbine-outlet plane, and radial total-temperature distributions are specified for this station. A typical total-temperature distribution at the turbine outlet for the short combustor in the full-scale engine is shown in figure 17. This distribution, having a moderate peak near the blade tip, was considered acceptable for this engine. It was obtained, however, only when all of the fuel was injected through the inner manifold of the dual fuel manifold. Since this engine also carried temperature instrumentation at

the combustor outlet, the temperature distributions upstream of the turbine could also be studied. As would be expected, with fuel injected from the inner manifold only, the radial temperature distribution at the combustor outlet had a high peak near the blade root. This radial-temperature distribution has some resemblance to that exhibited by the corresponding quarter-annulus-duct combustor (model 6) when operated in the same manner, as shown by the broken line in figure 17.

It is thus noted, from these studies with an engine instrumented at both the turbine inlet and outlet, that the radial total-temperature distribution into the turbine is consistent with that obtained at the combustor outlet of the quarter-annulus duct model. On the other hand, the temperature distribution into the turbine is almost the inverse of the distribution out of the turbine, or the desired distribution. If this observation is typical for many engines, the practice of using turbine-outlet profiles for design purposes may be misleading. The shift in temperature distribution through the turbine has been noted in previous studies (ref. 11), and it may be the result of flow-pattern changes through the rotor and stator passages and the discharge of turbine-disk cooling air into the exhaust gases.

4064

Combustor total-pressure loss. - Combustor total-pressure loss, in percent of combustor-inlet total pressure, is plotted in figure 18 as a function of the engine total-temperature ratio. Points are shown for corrected engine speeds of 100 and 96 percent of rated speed at a Reynolds number index of 0.08, conditions simulating those at about a 71,000-foot altitude at Mach 0.9. A curve representing the total-pressure loss of the quarter-annulus combustor, as a function of combustor total-temperature ratio (fig. 15), is included in figure 18. The measured pressure losses are comparable.

SUMMARY OF RESULTS

The following results were obtained from an investigation of a short channeled-wall combustor for hydrogen fuel in a quarter-annulus duct and from a comparison with the performance of a corresponding full-annulus combustor in a current, production-type turbojet engine:

1. Satisfactory performance at low pressures was achieved with a combustor liner consisting of a sheltered primary zone occupying about 20 percent of the cross-sectional area and a channeled-wall secondary zone. The best fuel-manifold design consisted of concentric spray bars situated between two V-gutter flameholders that were displaced longitudinally so that the fuel issued from the annular slots between the trailing edges of the V-gutters.

[redacted]

2. Combustion efficiency for the best configuration at fuel-air ratios of 0.007 to 0.009 ranged from 84 percent at a combustor-inlet total pressure of 5.7 inches of mercury absolute through 90 percent at 9.0 inches of mercury absolute to values approaching 100 percent at higher pressures. Combustor reference velocity had little effect on combustion efficiency at all pressures over a velocity range of 75 to 270 feet per second; the higher velocities were attained at pressures of 47 to 55 inches of mercury absolute, conditions simulating supersonic flight operation.

4064

3. By proportioning the fuel flow to the two manifolds of the dual fuel manifold, satisfactory control of the combustor-outlet radial-temperature distribution was achieved.

4. Combustor total-pressure loss ranged from 3.0 percent at isothermal conditions to 4.7 percent at a combustor total-temperature ratio of 3.6.

5. The full-annulus combustor that was scaled from the quarter-annulus duct models to fit a current, production-type annular turbojet engine operated at combustion efficiencies and total-pressure losses similar to those determined for the duct model. By means of the fuel distribution control, turbine-outlet total-temperature distributions in the engine were adjusted until an acceptable profile was obtained, without any alteration to the combustor liner. The length of the experimental combustor was approximately two-thirds of that of the production model.

Lewis Flight Propulsion Laboratory
National Advisory Committee for Aeronautics
Cleveland, Ohio, April 17, 1956

REFERENCES

1. Rothrock, Addison M.: Turbojet Propulsion-System Research and the Resulting Effects on Airplane Performance. NACA RM 54H23, 1955.

2. Olson, Walter T., and Gibbons, Louis C.: Status of Combustion Research on High-Energy Fuels for Ram Jets. NACA RM E51D23, 1951.

3. Silverstein, Abe, and Hall, Eldon W.: Liquid Hydrogen as a Jet Fuel for High-Altitude Aircraft. NACA RM E55C28a, 1955.

4. Lewis Flight Propulsion Laboratory: NACA Conference on Aircraft Propulsion Systems. 1955.

5. Coward, H. F., and Jones, G. W.: Limits of Inflammability of Gases and Vapors. Bull. 279, Bur. Mines, 1939.

6. Jonash, Edmund R., Smith, Arthur L., and Hlavin, Vincent F.: Low-Pressure Performance of a Tubular Combustor with Gaseous Hydrogen. NACA RM E54L30a, 1955.

7. Wear, Jerrold D., and Smith, Arthur L.: Performance of a Single Fuel-Vaporizing Combustor with Six Injectors Adapted for Gaseous Hydrogen. NACA RM E55I14, 1955.

8. Zettle, Eugene V., and Friedman, Robert: Performance of Experimental Channeled-Wall Annular Turbojet Combustor at Conditions Simulating High-Altitude Supersonic Flight. I - U-Shaped Channel Walls for Secondary-Air Entry. NACA RM E54L21a, 1955.

9. Friedman, Robert, and Carlson, Edward R.: A Polar-Coordinate Survey Method for Determining Jet-Engine Combustion-Chamber Performance. NACA TN 3566, 1955.

10. Childs, J. Howard, and Graves, Charles C.: Relation of Turbine-Engine Combustion Efficiency to Second-Order Reaction Kinetics and Fundamental Flame Speed. NACA RM E54G23, 1954.

11. Mark, Herman, and Zettle, Eugene V.: Axial-Slot Air Admission for Controlling Performance of a One-Quarter-Annulus Turbojet Combustor and Comparison with Complete Engine. NACA RM E52A21, 1952.

TABLE I. - EXPERIMENTAL DATA

Run	Combustor-inlet total pressure, in. Hg abs	Combustor-inlet total temperature, °R	Air-flow rate, lb/sec	Combustor reference velocity, ft/sec	Fuel-flow rate, lb/hr	Fuel-air ratio	Mean combustor-outlet temperature, °R	Mean temperature rise, °F	Combustion efficiency, percent	Inlet fuel temperature, °F	Fuel-manifold pressure, in. Hg abs		Approx. percent fuel to outer manifold	Total-pressure drop through combustor, percent
											Manifold			
											Outer	Inner		
Model 1 (Single manifold, single gutter)														
1	5.7	543	0.75	74.0	17.9	6.64×10^{-3}	1482	918	71.8	69	19		---	2.8
2	5.7	544	.75	74.0	25.8	8.70	1684	1140	70.5	70	23		---	---
3	5.7	544	.99	97.5	25.8	6.68	1485	921	71.7	69	23		---	---
4	5.7	544	.99	97.5	30.9	8.68	1710	1166	72.3	68	29		---	---
5	5.7	544	1.155	112.0	26.5	5.45	1280	736	68.0	66	25		---	---
6	5.8	544	1.155	110.0	39.8	8.15	1583	1019	86.2	63	37		---	---
7	9.0	544	1.17	73.0	22.9	5.44	1390	846	78.8	62	24		---	---
8	9.0	544	1.17	73.0	31.6	7.50	1671	1127	82.5	60	29		---	---
9	9.0	544	1.83	95.5	31.3	5.68	1419	875	78.9	60	29		---	---
10	9.0	543	1.55	95.5	49.3	8.98	1767	1224	73.8	54	45		---	---
Model 2 (Twin manifold, single gutter)														
1	5.7	540	0.75	73.7	17.9	6.85×10^{-3}	1502	1052	84.5	74	18		---	---
2	5.7	540	.75	73.7	23.6	8.74	1836	1296	80.5	76	18		---	---
3	9.0	541	1.17	72.8	25.0	5.46	1590	1049	100.0	74	17		---	---
4	9.0	541	1.17	72.8	31.8	7.48	1798	1257	80.0	72	21		---	---
Model 3 (Single manifold, double gutter)														
1	5.7	548	0.75	74.5	23.1	8.45×10^{-3}	1988	1440	95.5	86	24		---	---
2	5.7	548	.75	74.5	31.4	11.48	2254	1606	85.0	87	29		---	---
3	9.0	548	1.17	73.6	29.3	6.98	1808	1260	97.2	84	27		---	---
4	9.0	548	1.17	73.6	38.4	8.65	2010	1462	92.9	82	35		---	---
Model 4 (Dual manifold, double gutter)														
1	5.7	538	0.75	73.0	18.2	6.74×10^{-3}	1444	906	70.0	56	14	16	50	3.4
2	5.7	538	.75	73.0	24.3	9.00	1885	1147	70.2	58	17	19	50	3.4
3	5.7	536	.75	73.0	24.2	8.98	1708	1170	71.8	52	19	19	40	3.5
4	5.7	536	.75	73.0	24.5	9.08	1749	1213	75.3	50	15	21	25	3.5
5	5.7	537	.75	73.0	24.2	8.96	1743	1206	74.2	46	9	27	10	3.5
6	6.0	537	1.35	125.0	40.8	8.39	1612	1075	89.4	42	27	28	50	12.4
7	6.0	538	1.35	125.0	40.7	8.37	1605	1069	89.3	45	28	28	25	10.0
Model 5 (Dual manifold, double gutter)														
1	5.7	543	0.75	74.0	25.6	8.74×10^{-3}	1672	1129	69.9	60	18	15	50	---
2	5.7	543	.75	74.0	15.6	5.05	1302	759	77.6	60	14	9	50	---
3	5.7	542	.75	74.0	17.7	6.54	1521	979	78.2	68	13	11	50	---
4	5.7	543	.75	74.0	11.6	4.28	1344	701	82.8	68	11	8	60	---
5	5.7	544	.75	74.0	21.7	8.37	1675	1128	72.8	68	14	13	50	---
6	5.7	544	.75	74.0	17.8	6.87	1474	930	73.8	67	21	5	100	---
7	5.7	544	.75	74.0	17.8	6.87	1459	1095	88.2	68	9	22	0	---
Model 6 (Dual manifold, double gutter)														
1	5.7	539	0.75	73.2	11.5	4.20×10^{-3}	1271	732	87.2	72	15	8	50	---
2	5.7	539	.75	73.2	17.5	6.39	1582	1023	83.4	74	13	11	50	---
3	5.7	540	.75	73.2	21.5	7.85	1688	1148	77.4	74	15	13	50	---
4	5.7	540	.75	73.2	11.3	4.15	1302	782	92.3	72	9	14	0	---
5	5.7	540	.75	73.2	17.5	6.38	1573	1033	84.3	71	9	22	0	---
6	5.7	540	.75	73.2	17.7	6.45	1500	960	81.0	70	22	0	100	---
7	5.7	541	.99	96.4	17.8	4.11	1252	711	86.8	87	24	8	100	---
8	5.7	541	.99	96.4	17.7	4.09	1252	721	89.8	88	18	12	50	---
9	5.7	540	.99	96.4	23.7	5.47	1443	903	86.3	64	18	16	50	---
10	5.7	540	.99	96.4	28.9	6.69	1667	1127	88.8	60	11	19	50	---

TABLE I. - Concluded. EXPERIMENTAL DATA

Run	Combustor-inlet total pressure, in. Hg abs	Combustor-inlet total temperature, t_R	Air-flow rate, lb/sec	Combustor reference velocity, ft/sec	Fuel-flow rate, lb/hr	Fuel-air ratio	Mean combustor-outlet temperature, t_R	Mean temperature rise, ^oF	Combustion efficiency, percent	Inlet fuel temperature, ^oF	Fuel-manifold pressure, in. Hg abs		Approx. percent fuel to outer manifold	Total-pressure drop through combustor, percent
											Manifold			
											Outer	Inner		
Model 7 (Dual manifold, double gutter)														
1	5.7	532	0.76	73.8	18.2	6.64×10^{-3}	1654	1122	87.6	60	13	11	80	----
2	5.7	536	.76	73.8	18.1	6.66	1508	972	85.8	62	21	5	100	----
3	5.7	538	.76	74.0	18.1	6.85	1617	1079	84.4	61	18	7	80	----
4	5.7	539	.75	73.4	10.0	3.72	1233	694	92.1	62	13	8	80	1.8
5	5.7	539	.75	73.4	12.7	4.72	1386	757	90.0	61	14	8	80	1.8
6	5.7	540	.75	73.5	21.8	8.07	1822	1282	84.7	60	20	7	80	1.8
7	5.7	540	.75	73.5	23.9	8.85	1905	1365	83.4	59	21	8	80	1.8
8	5.7	541	.98	98.5	16.2	4.59	1360	819	92.3	59	18	8	80	10.5
9	5.7	540	.98	96.5	24.0	6.80	1621	1081	84.2	58	23	8	80	10.8
10	5.7	540	.98	96.5	29.1	8.24	1864	1324	79.3	57	25	9	80	10.5
11	5.7	540	1.30	127.5	22.2	4.76	1352	812	85.9	56	21	7	80	11.4
12	5.7	540	1.30	127.5	32.0	6.85	1625	1085	83.7	54	27	9	80	11.4
13	5.7	540	1.30	127.5	38.2	8.18	1793	1253	81.8	53	30	11	80	12.3
14	6.1	540	1.84	141.0	38.5	8.95	1660	1120	84.0	51	30	11	80	----
15	9.0	540	1.17	72.5	17.0	4.04	1319	779	98.2	58	19	9	80	4.5
16	9.0	540	1.17	72.5	20.2	4.80	1407	867	91.0	55	19	10	80	4.5
17	9.0	540	1.17	72.5	28.2	6.70	1721	1281	92.4	52	25	11	80	5.8
18	9.0	540	1.17	72.5	34.9	8.30	1927	1387	80.1	50	29	12	80	5.5
19	9.0	540	1.52	94.2	36.2	6.98	1780	1240	93.5	44	31	12	80	----
20	9.0	540	2.08	129.0	50.1	8.69	1735	1195	85.9	41	34	15	80	18.4
21	15.0	535	1.94	71.3	28.9	4.14	1411	876	103.7	50	29	15	80	3.2
22	15.0	534	1.94	71.3	49.0	7.02	1919	1385	102.5	50	33	19	80	3.5
23	15.0	534	1.94	71.3	60.0	8.60	2171	1637	102.5	48	38	22	80	3.8
24	15.0	534	2.59	95.5	65.9	7.07	1780	1256	98.7	47	36	22	80	7.3
25	15.0	534	3.26	120.5	78.9	6.72	1765	1229	98.5	42	40	25	80	12.9
26	30.0	535	3.90	71.8	57.0	4.06	1359	828	98.1	41	35	30	80	3.9
27	30.0	532	3.90	71.8	72.5	5.18	1587	1055	98.4	38	38	31	80	4.0
28	30.0	533	3.90	71.6	93.0	6.62	1845	1312	96.8	35	45	31	80	4.5
29	15.0	535	1.95	71.8	----	----	(Cold flow)		----	--	--	--	--	----
30	15.0	535	2.60	96.0	----	----	(Cold flow)		----	--	--	--	--	8.1
31	15.0	535	3.26	120.0	----	----	(Cold flow)		----	--	--	--	--	8.1
32	15.0	532	3.91	144.0	----	----	(Cold flow)		----	--	--	--	--	14.5
33	30.0	532	3.91	71.8	----	----	(Cold flow)		----	--	--	--	--	3.1
Model 8 (Dual manifold, double gutter)														
1	5.7	535	0.75	73.0	12.6	4.74×10^{-3}	1425	890	96.3	50	14	6	80	3.9
2	5.7	537	.75	73.1	18.4	6.85	1755	1198	93.2	47	20	7	80	----
3	5.7	537	.75	73.1	22.1	8.18	1808	1369	91.2	47	23	8	80	----
4	5.7	538	.75	73.3	18.4	6.85	1745	1207	94.0	45	15	12	80	----
5	5.7	538	.75	73.3	18.4	6.85	1728	1188	92.2	44	24	5	100	----
6	15.0	540	1.98	73.6	----	----	(Cold flow)							
7	15.0	540	1.98	73.6	27.4	5.84	1408	865	114.0	58	22	21	50	3.9
8	15.0	541	1.98	73.6	36.3	6.09	1679	1138	116.0	60	26	25	50	3.7
9	15.0	542	1.98	73.7	45.8	6.86	1950	1408	116.0	56	29	30	50	4.7
10	15.0	543	1.98	73.8	58.5	8.34	2195	1652	109.0	49	32	32	50	4.3
11	15.0	1220	1.90	160	----	----	(Cold flow)		----	--	--	--	----	8.5
12	15.0	1205	2.40	195	----	----	(Cold flow)		----	--	--	--	----	10.5
13	15.0	1220	2.97	250	----	----	(Cold flow)		----	--	--	--	----	21.0
14	15.0	1215	2.40	202	----	----	(Cold flow)		----	--	--	--	----	8.4
15	15.0	1220	2.39	201	28.4	3.31	1851	631	97.0	28	22	22	50	10.8
16	15.0	1195	2.39	197	40.4	4.70	2024	829	95.5	25	29	27	50	11.8
17	15.0	1220	2.38	201	67.8	7.87	2404	1184	88.8	18	32	32	50	13.8
18	15.0	1205	3.00	250	----	----	(Cold flow)		----	--	--	--	--	----
19	15.0	1205	2.98	250	45.4	4.21	1919	714	85.0	18	29	29	50	----
20	55.1	1355	9.00	229	85.2	2.57	1900	545	103.5	30	39	39	50	----
21	55.6	1340	9.05	225	181.0	5.68	2378	1038	99.0	31	50	50	50	----
22	47.0	1355	9.00	288	192.0	5.93	2378	1023	97.6	18	50	50	50	----
23	47.0	1355	9.00	288	249.0	7.70	2658	1303	90.5	5	57	57	50	----

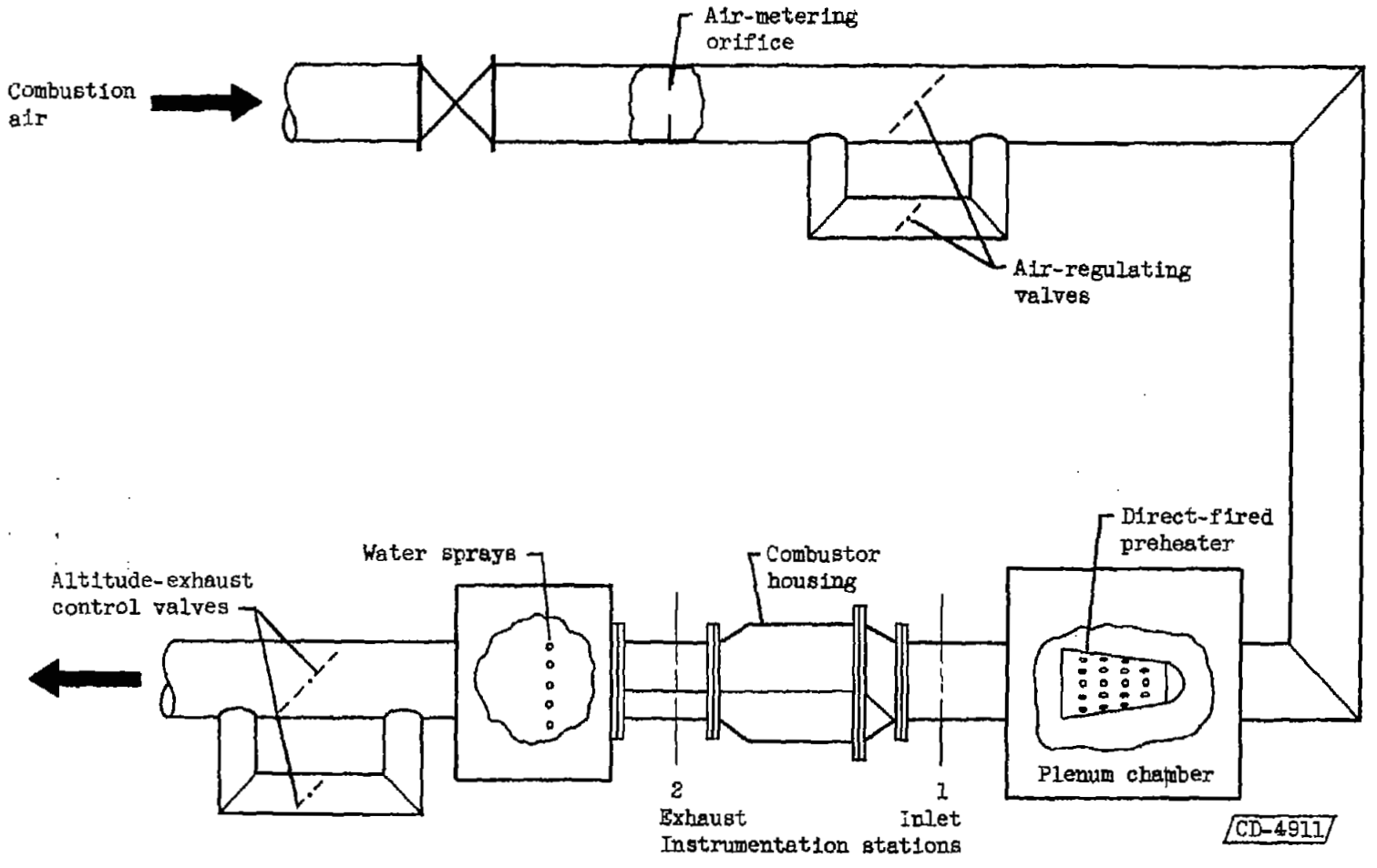

Figure 1. - Installation of one-quarter-annulus combustor.

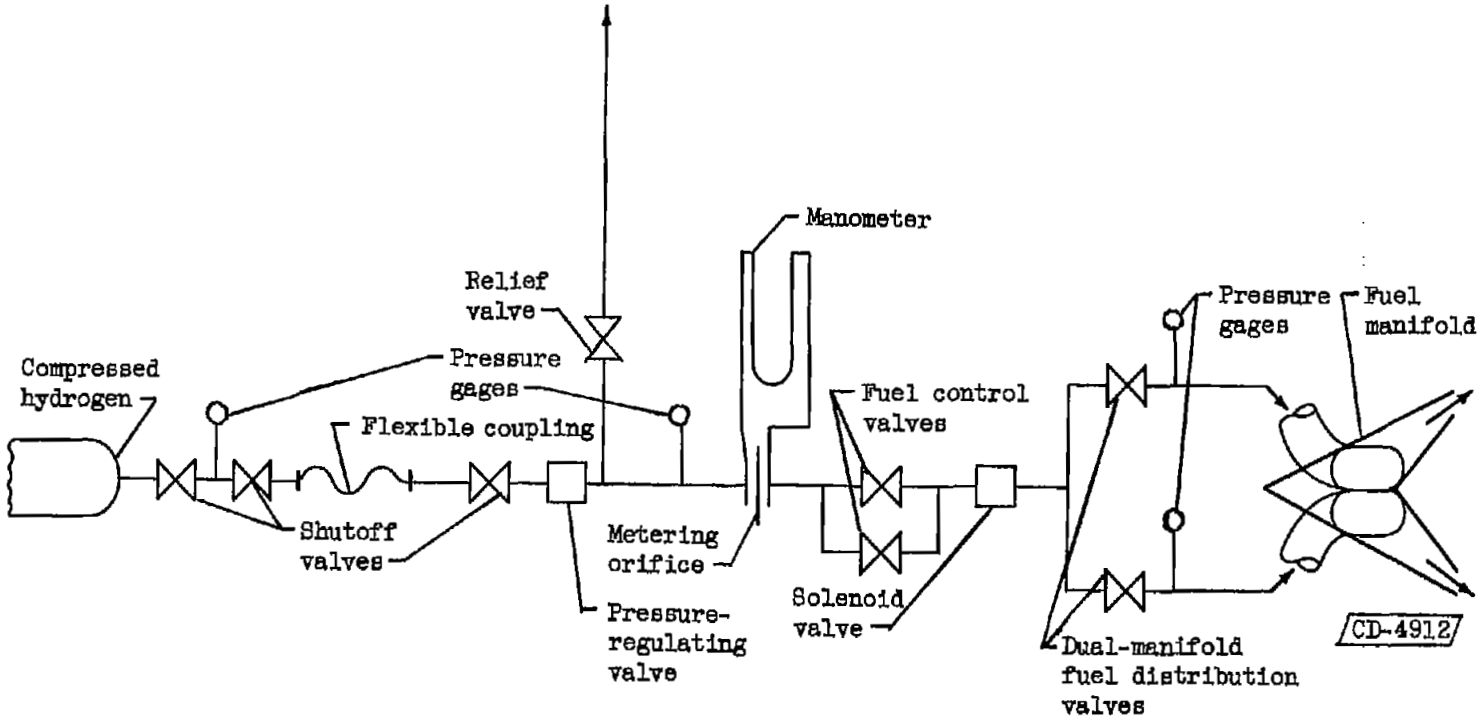

Figure 2. - Schematic diagram of hydrogen-fuel system.

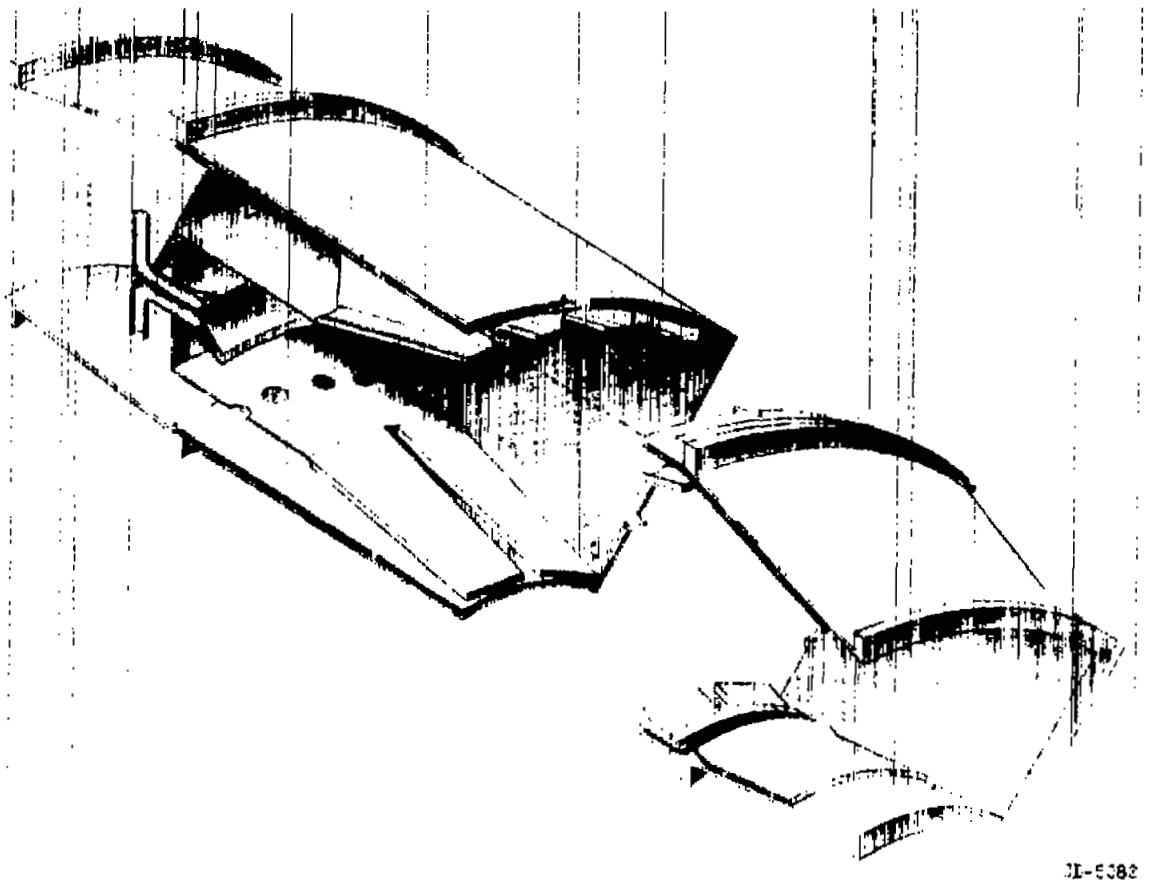

E-9382

Figure 3. - Three-quarter-cutaway view of final combustor configuration, model 8, assembled in quarter-annulus test ducting.

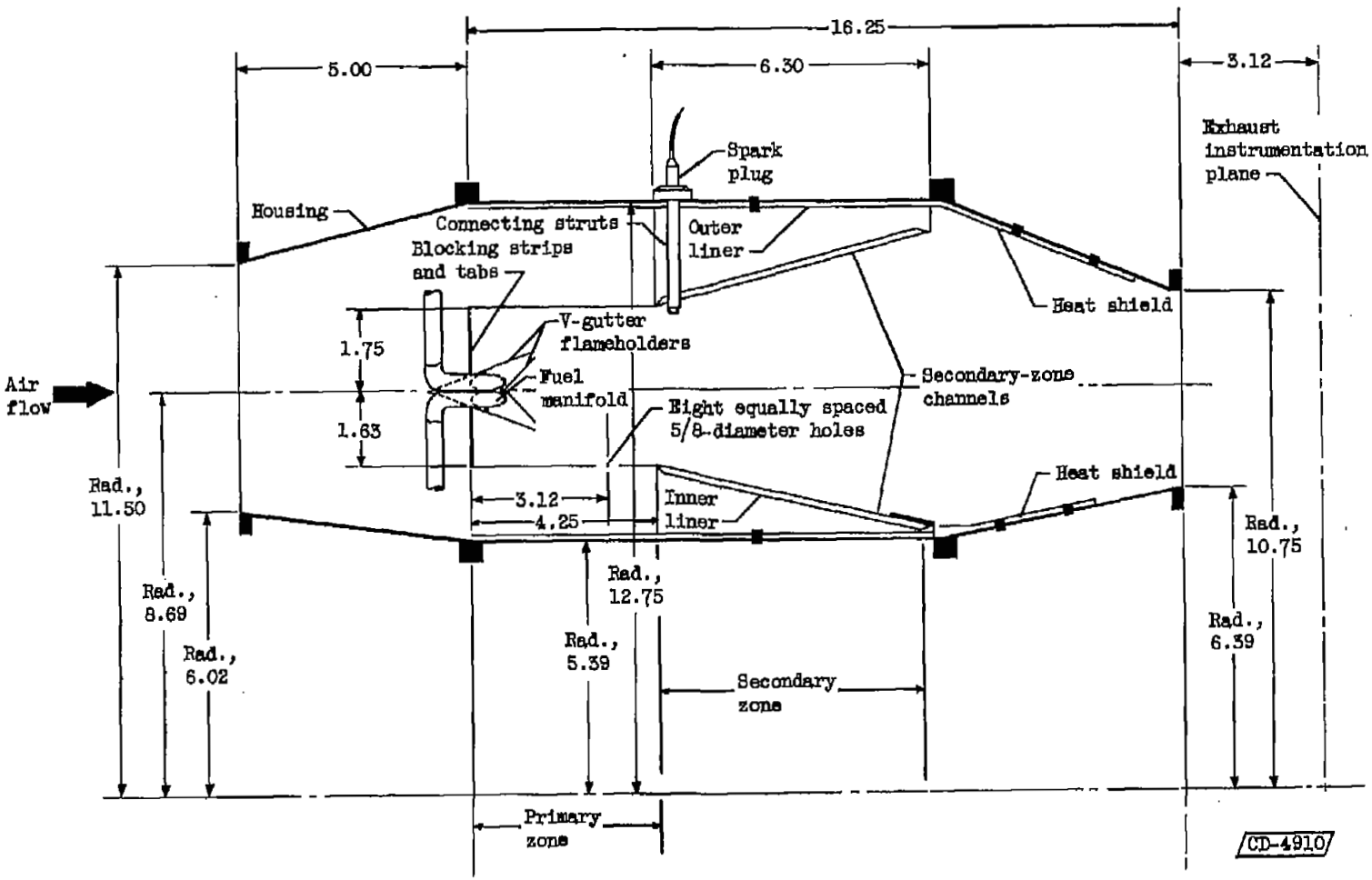

Figure 4. - Cross-sectional view of final combustor configuration, model 8, assembled in quarter-annulus test ducting. (All dimensions in inches.)

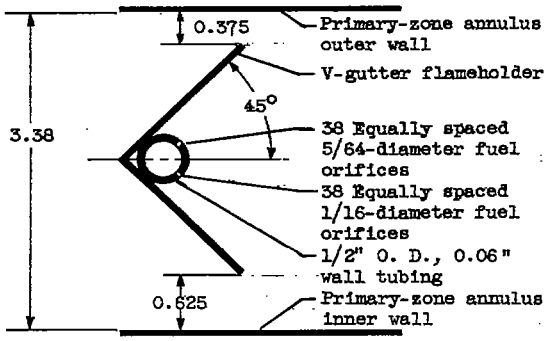

(a) Model 1. Longitudinal cross section through primary zone.

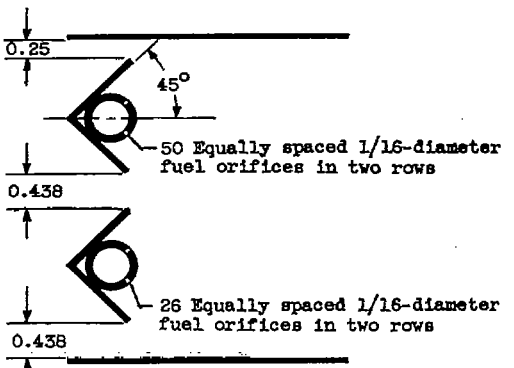

(b) Model 2. Longitudinal cross section through primary zone.

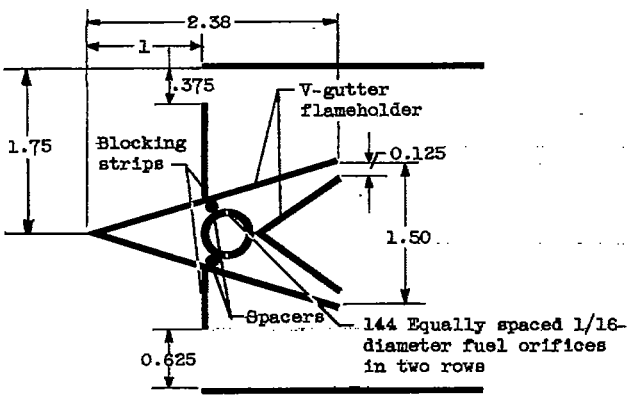

(c) Model 3. Longitudinal cross section through primary zone.

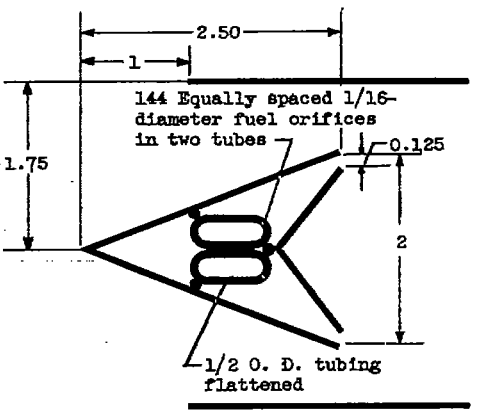

(d) Model 4. Longitudinal cross section through primary zone.

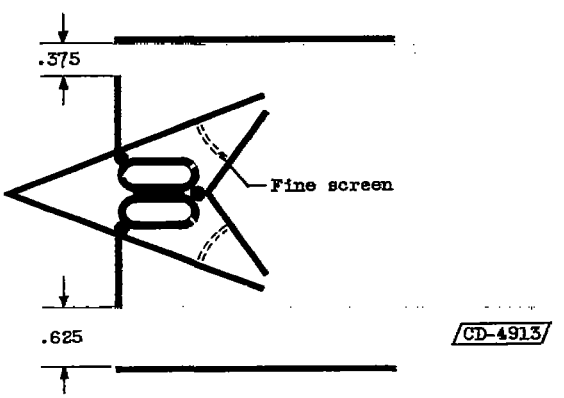

(e) Model 5. Longitudinal cross section through primary zone.

Figure 5. - Sketches of manifolds and liners of combustor models 1 to 8. (All dimensions in inches.)

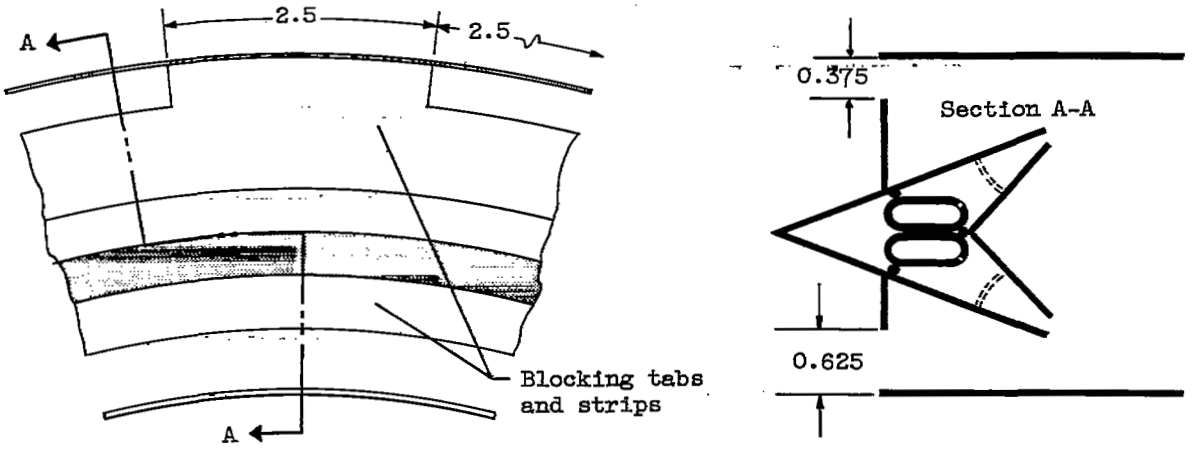

(f) Model 6. Upstream end view and longitudinal cross section through primary zone.

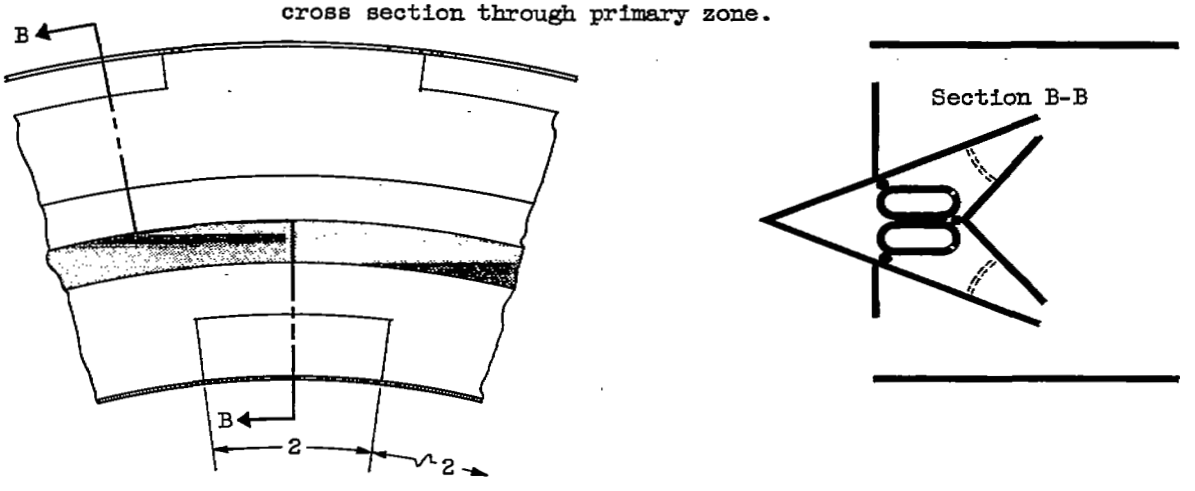

(g) Model 7. Upstream end view and longitudinal cross section through primary zone.

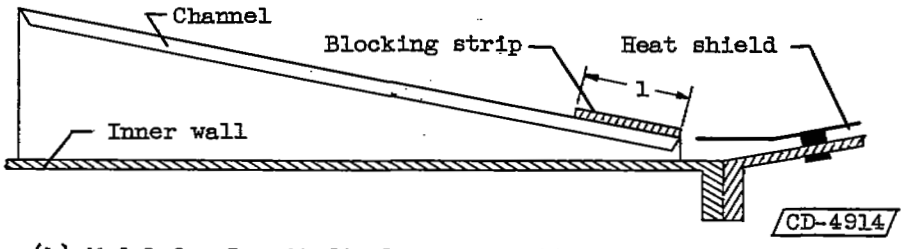

(h) Model 8. Longitudinal cross section through inner wall of secondary zone.

Figure 5. - Concluded. Sketches of manifolds and liners of combustor models 1 to 8. (All dimensions in inches.)

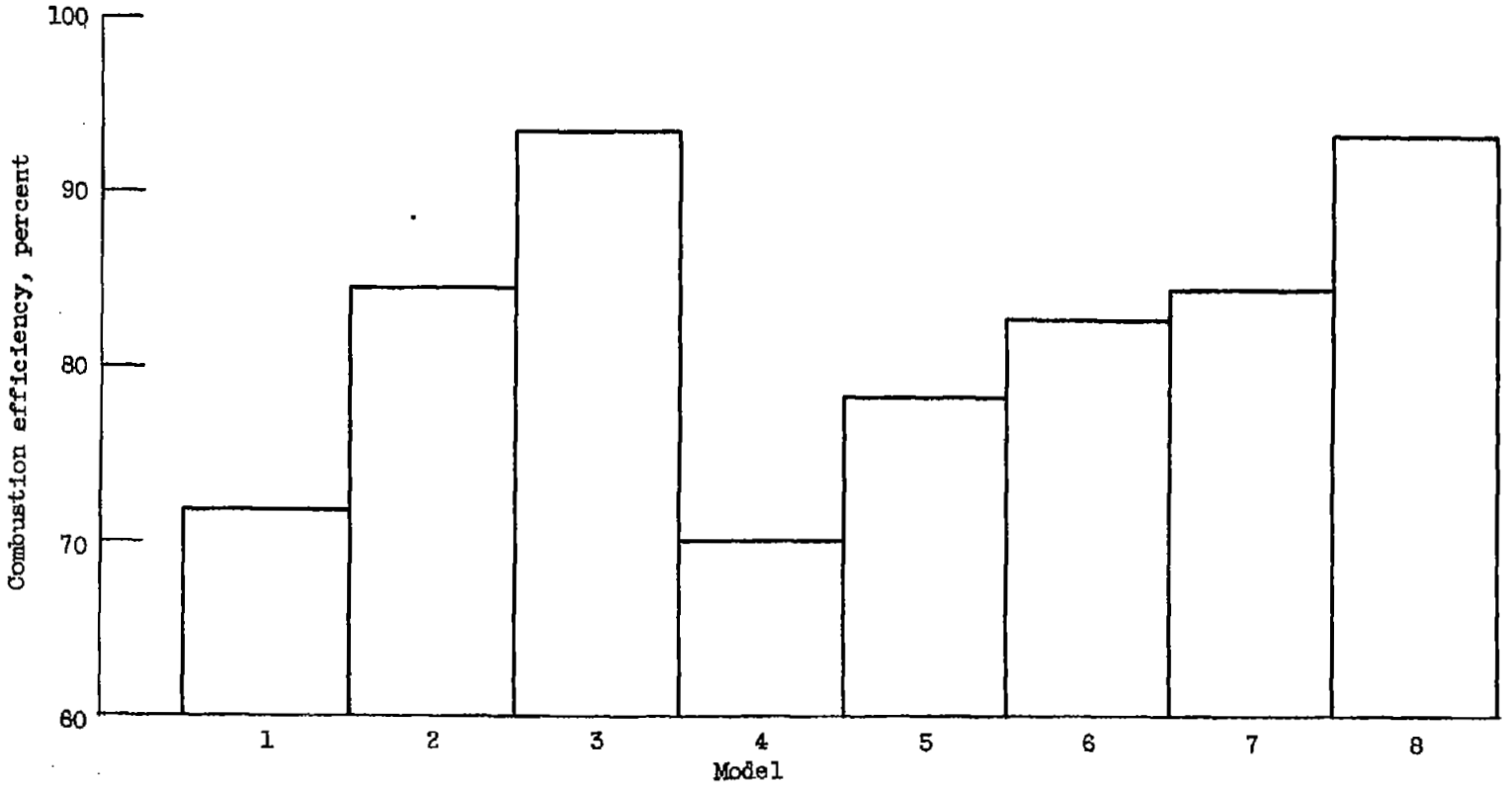

Figure 6. - Combustion efficiency for eight combustor models. Inlet-air total pressure, 5.7 inches of mercury absolute; inlet-air total temperature, 80° F; reference velocity, 80 feet per second; fuel-air ratio, 0.0066, except for model 3 (fuel-air ratio, 0.0085).

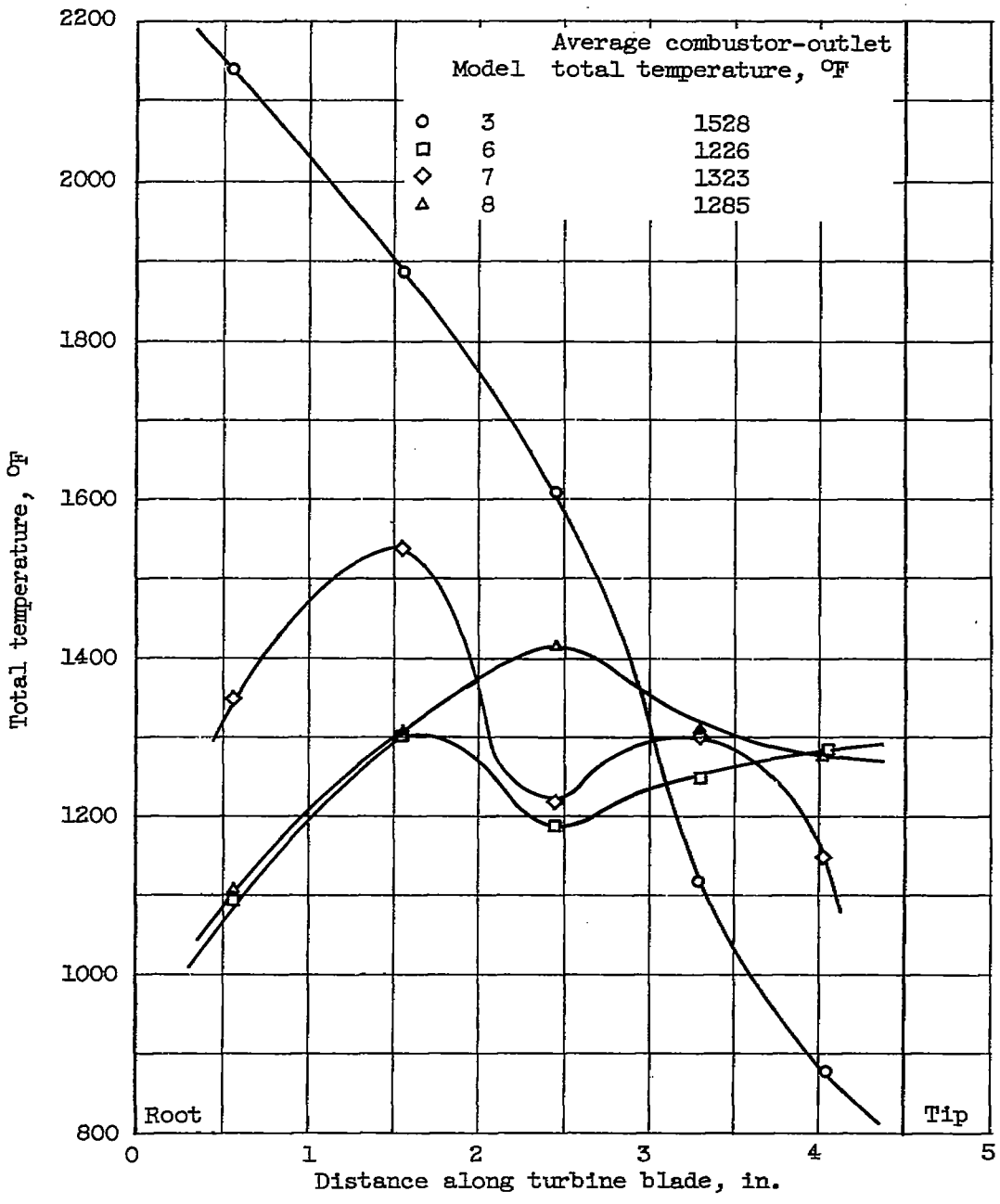

Figure 7. - Comparison of radial temperature distribution at combustor-exhaust plane for selected models. Inlet-air total pressure, 5.7 inches of mercury absolute; inlet-air temperature, 80° F; reference velocity, 80 feet per second; fuel-air ratio, 0.007 to 0.008; models 6, 7, and 8 operated with equal fuel distribution to both manifolds.

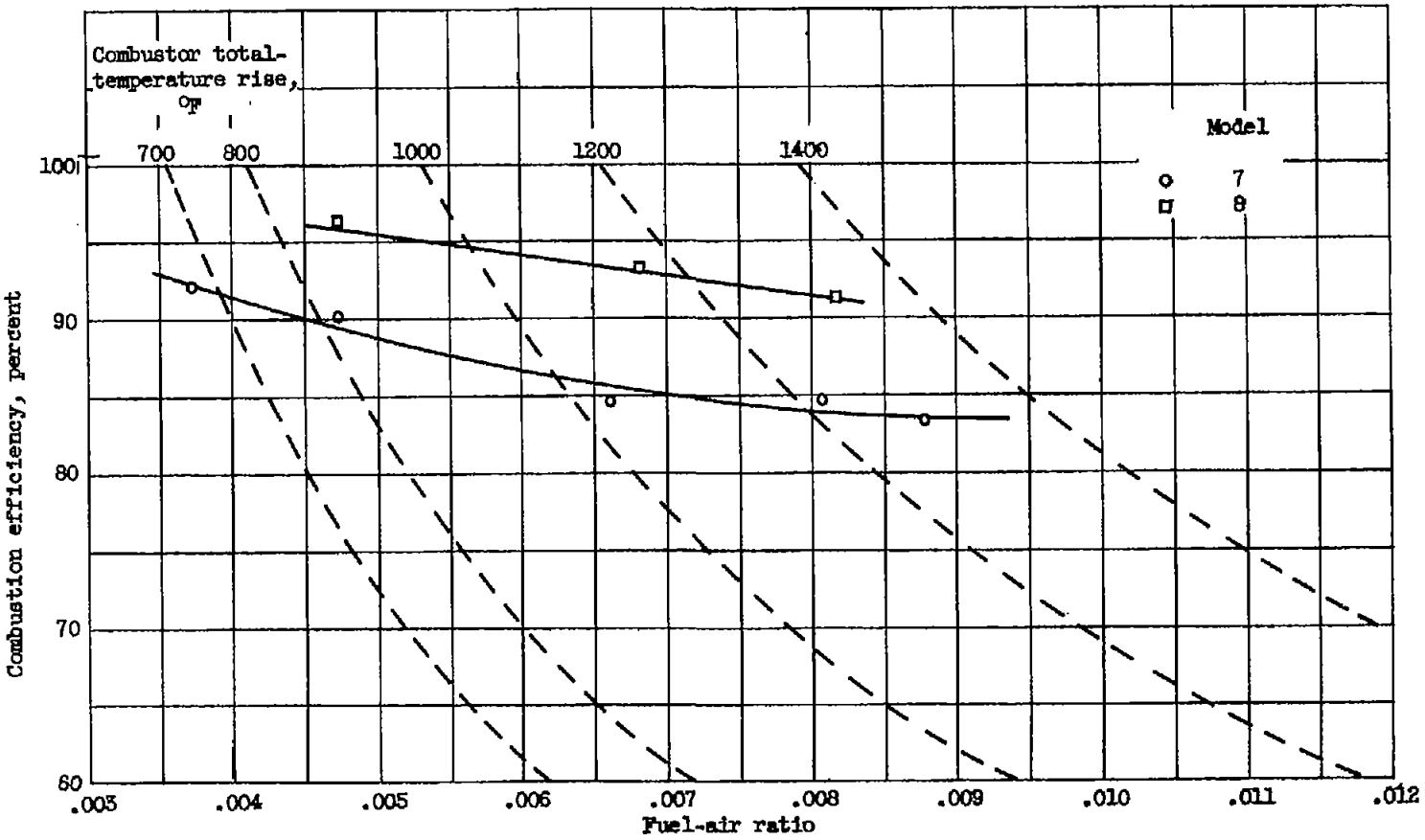

Figure 8. - Combustion efficiency of final combustor models. Inlet-air total pressure, 5.7 inches of mercury absolute; inlet-air total temperature, 80° F; reference velocity, 80 feet per second.

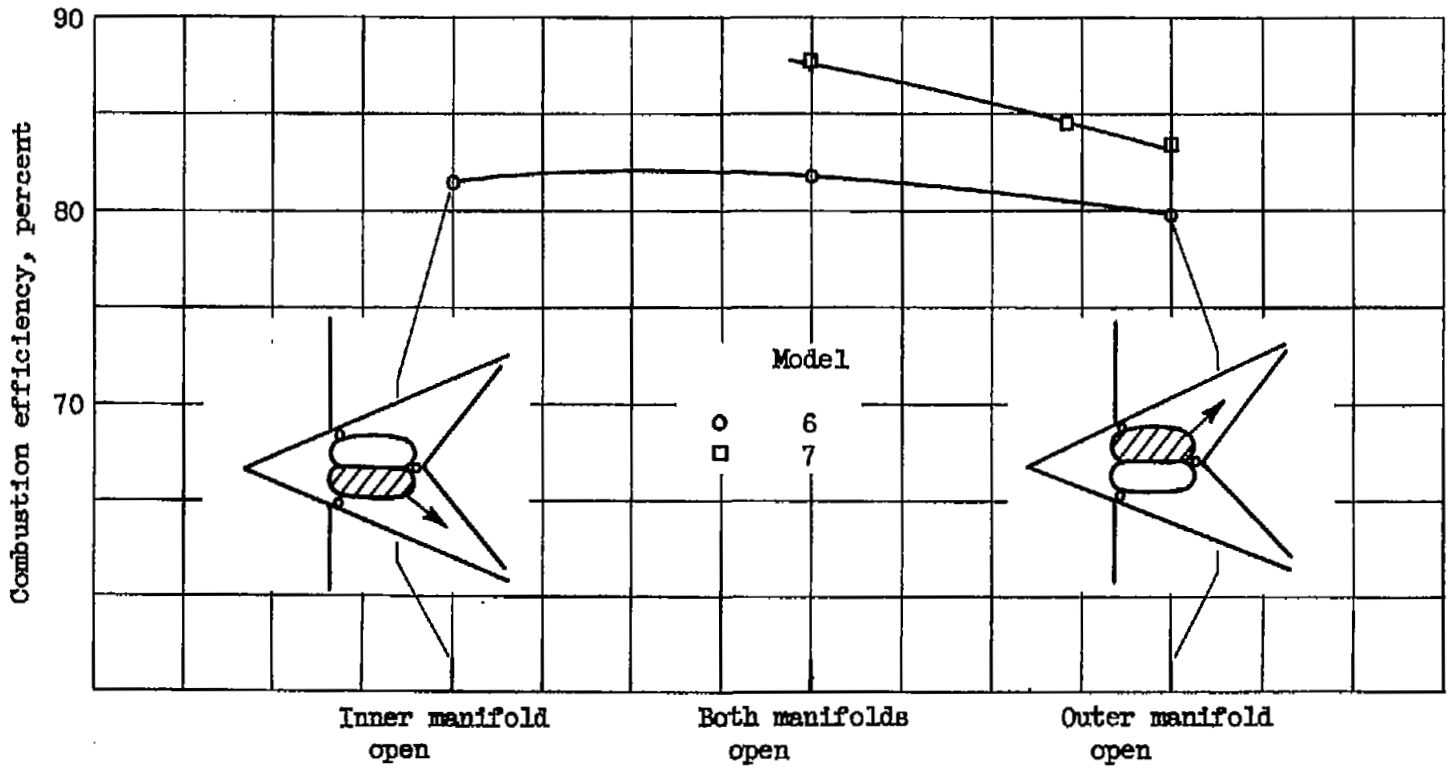

Figure 9. - Effect of variation of fuel distribution to dual fuel manifold on combustion efficiency. Inlet-air total pressure, 5.7 inches of mercury absolute; inlet-air total temperature, 80° F; reference velocity, 80 feet per second; fuel-air ratio, 0.0066.

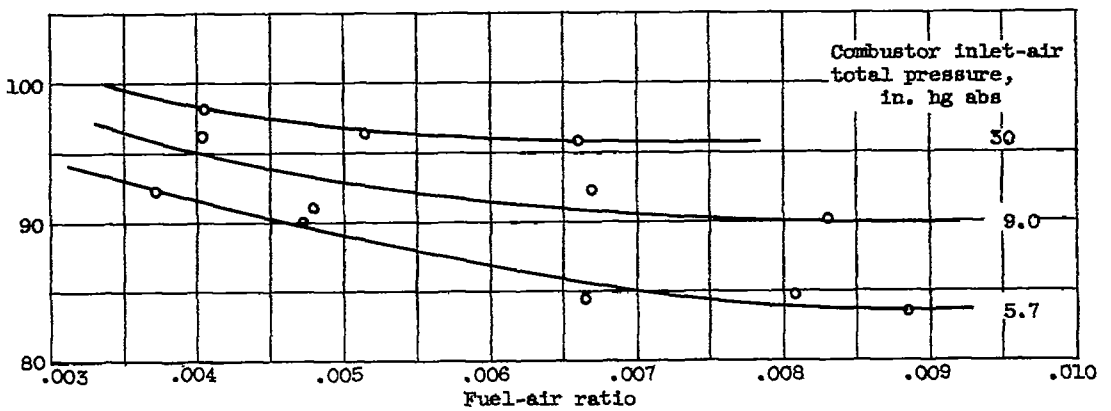

Figure 10. - Combustion efficiency of model 7 at several pressures. Inlet-air total temperature, 80° F; reference velocity, 80 feet per second.

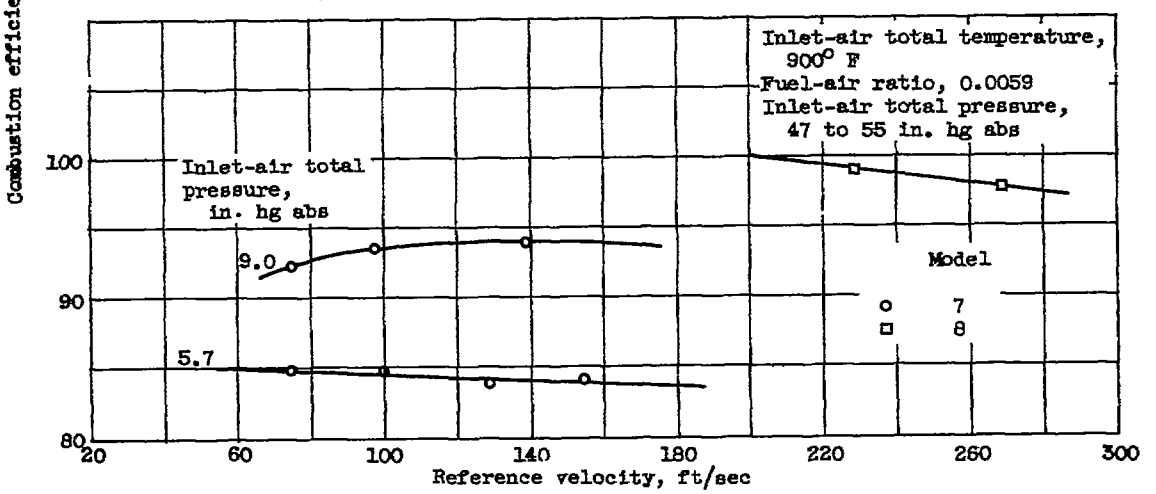

Figure 11. - Effect of reference velocity on combustion efficiency of models 7 and 8. Inlet-air total temperature, 80° F; fuel-air ratios, 0.0067 to 0.0070, except as noted.

[redacted]

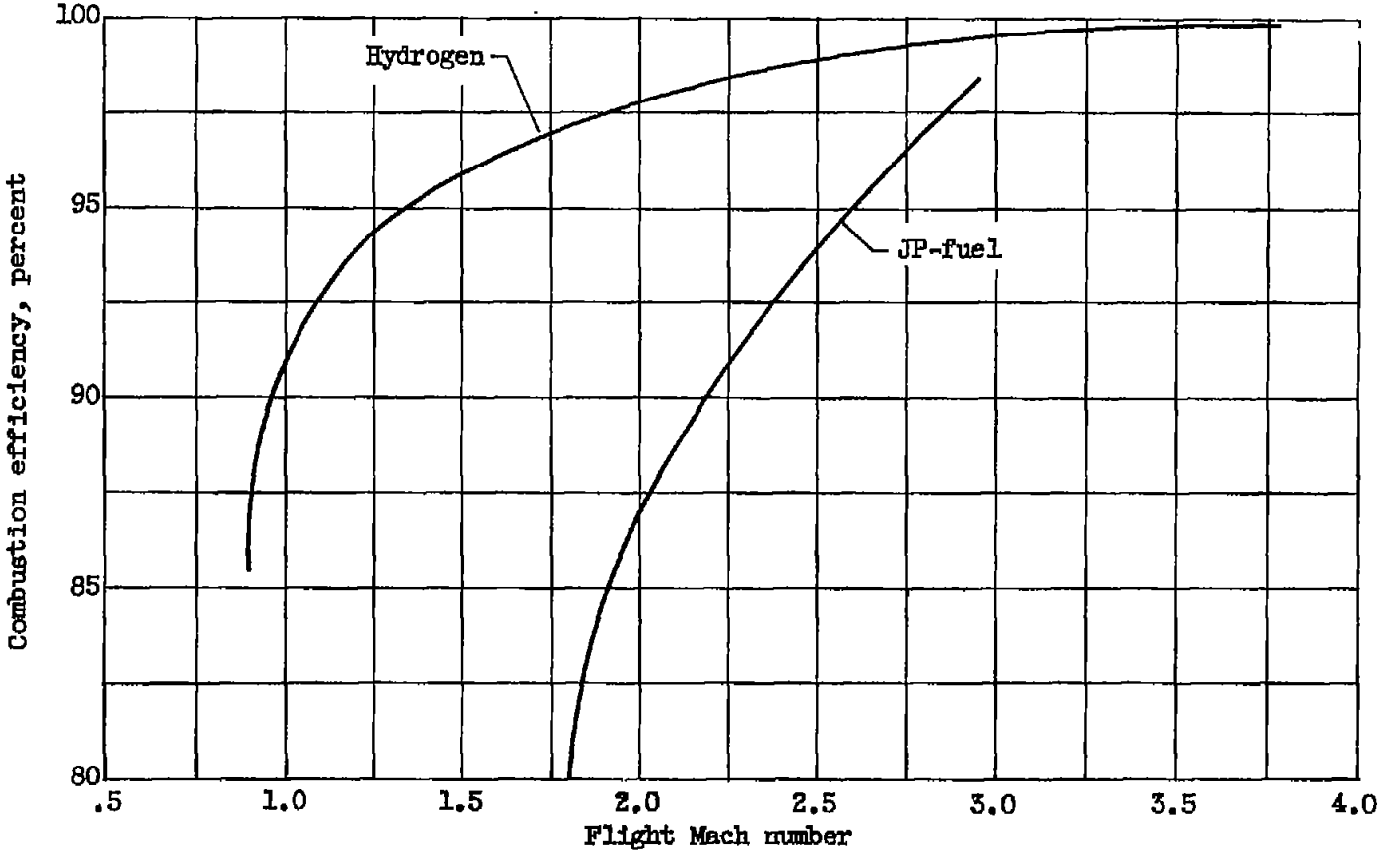

Figure 12. - Comparison of combustion efficiency of model 8 using hydrogen fuel with a corresponding channelled-wall combustor using JP-type fuel (ref. 4). Simulated flight Mach number calculated for engine with sea-level-static compressor total-pressure ratio of 4.2 at flight altitude of 80,000 feet; hydrogen-fuel combustor was 25 percent shorter than JP-fuel combustor.

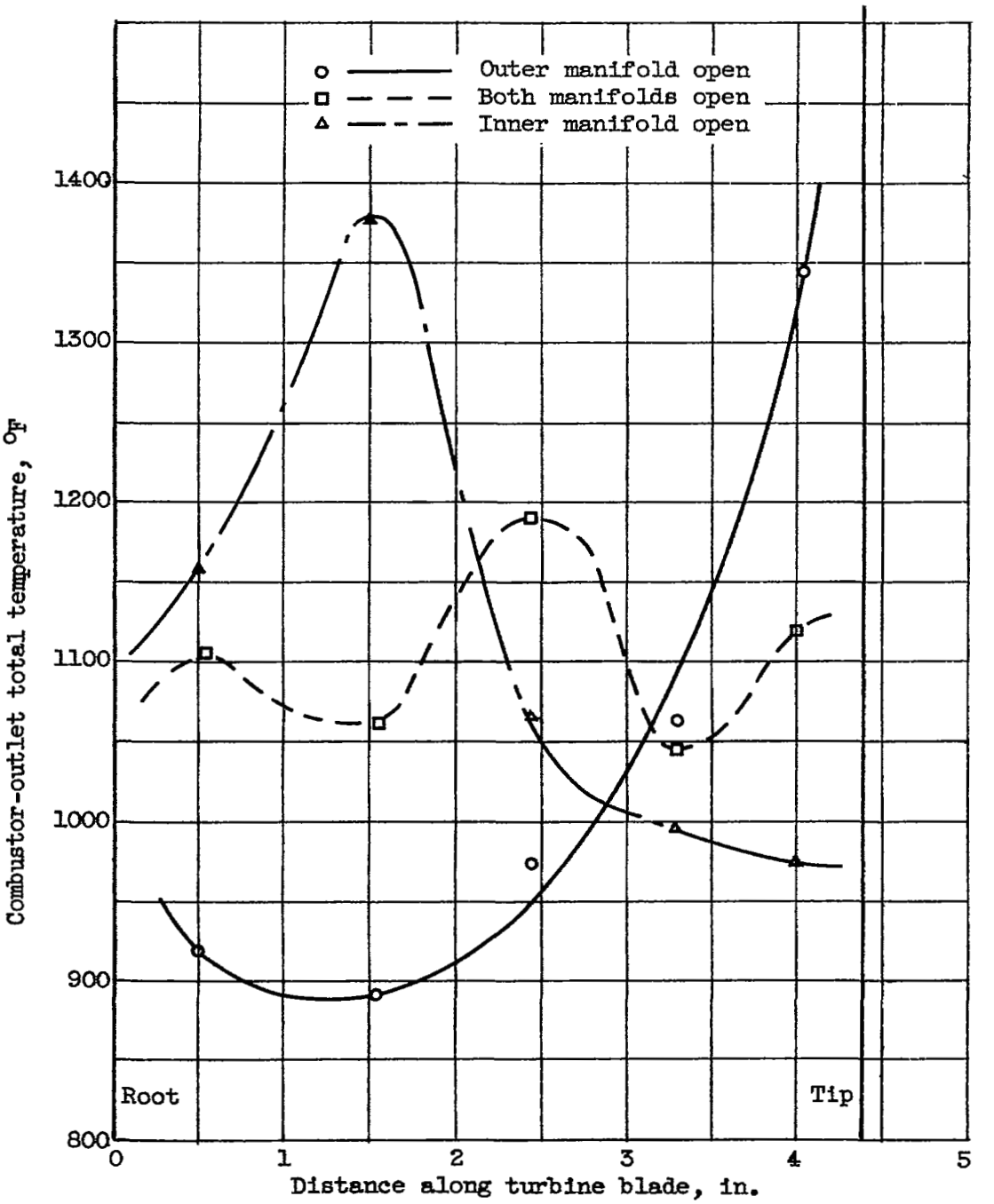

Figure 13. - Effect of fuel distribution to dual fuel manifold on outlet radial total-temperature profile for model 6. Inlet-air total pressure, 5.7 inches of mercury absolute; inlet-air total temperature, 80° F; reference velocity, 80 feet per second; fuel-air ratio, 0.0064.

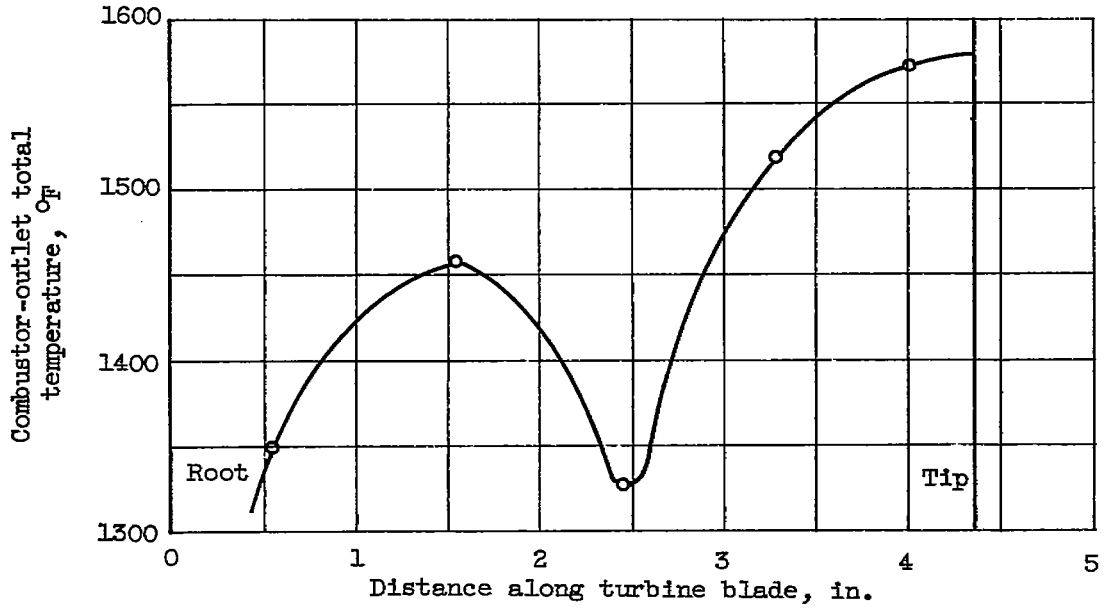

Figure 14. - Outlet radial total-temperature profile for final configuration, model 7. Inlet-air total pressure, 5.7 inches of mercury absolute; inlet-air total temperature, 80° F; reference velocity, 80 feet per second; fuel-air ratio, 0.0089; average outlet total temperature, 1445° F; fuel-flow distribution, 80 percent to outer manifold.

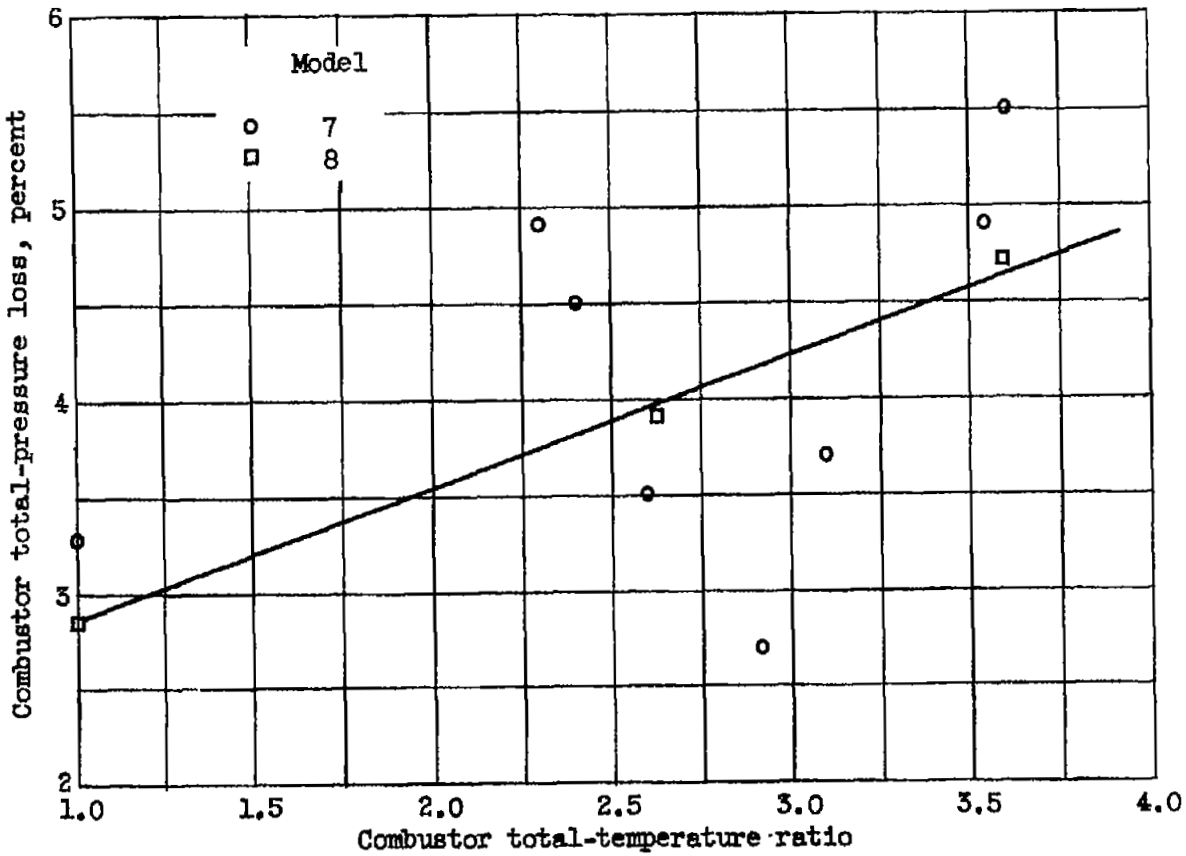

Figure 15. - Combustor total-pressure loss for models 7 and 8 in the quarter-annulus duct. Reference velocity, 80 feet per second.

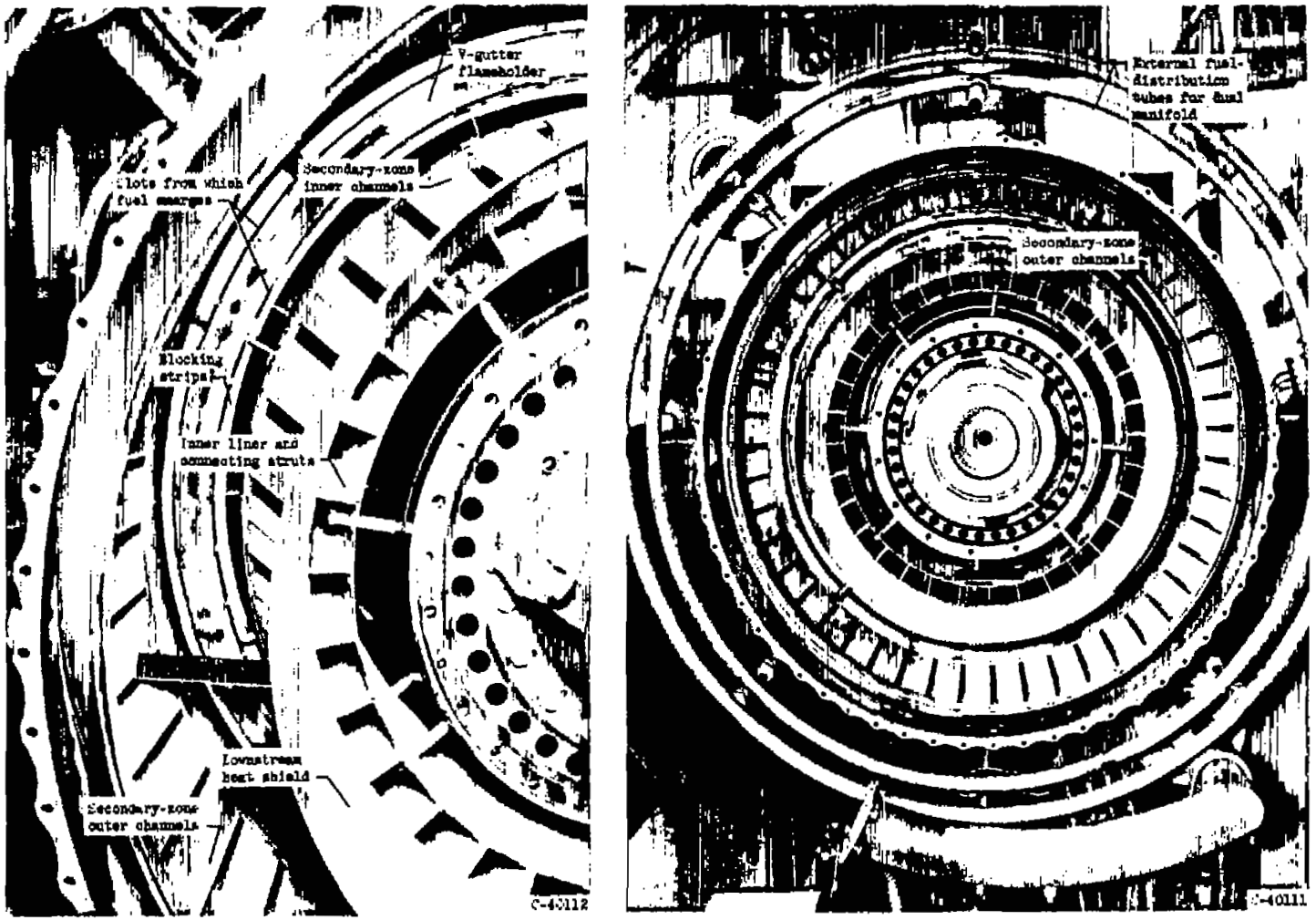

(a) Enlargement of details.

(b) Over-all view.

Figure 16. - Photographs of hydrogen-fuel combustor in full-scale engine, looking upstream from turbine nozzle diaphragm. Combustor design based on model 6.

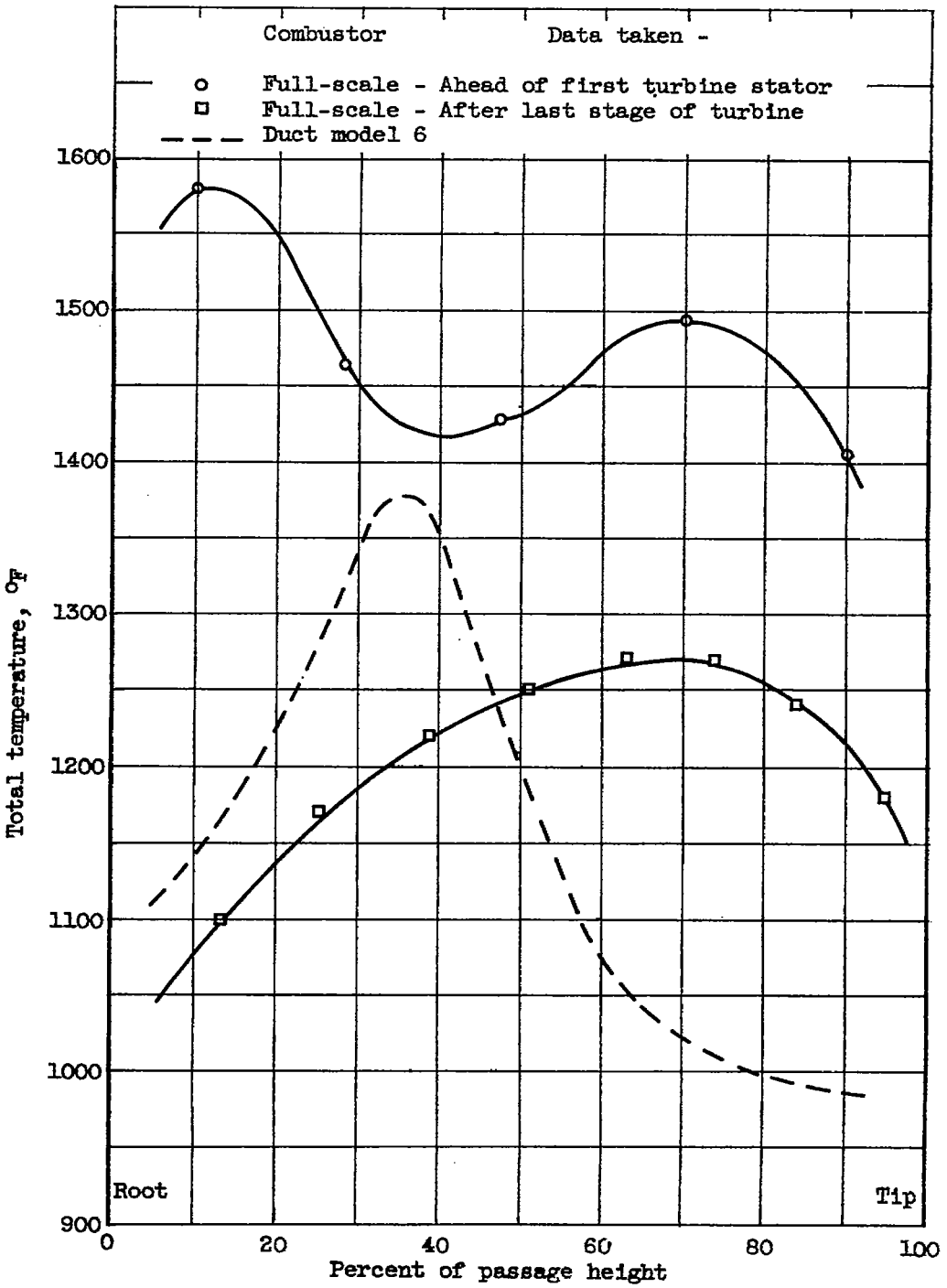

Figure 17. - Comparison of full-scale and quarter-annulus-duct outlet total-temperature profiles. Outer manifolds closed.

[redacted]

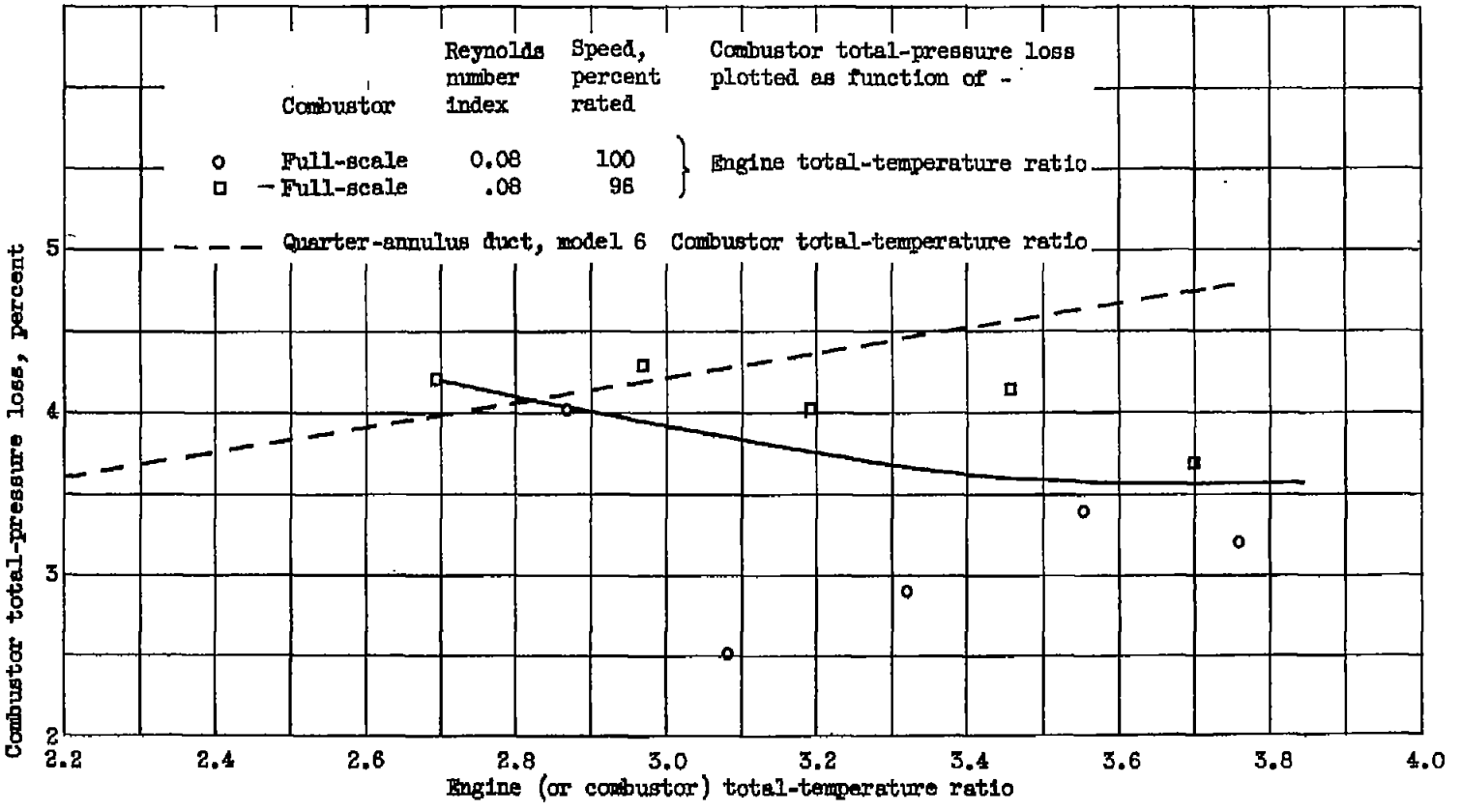

Figure 18. - Comparison of combustor total-pressure loss for full-scale and quarter-annulus combustors.